TECHNISCHE UNIVERSITÄT WIEN
Vienna University of Technology

institute of telecommunications

Master Thesis

Measurement Based Evaluation of the Wireless Identification and Sensing Platform

Performed for the purpose of obtaining the academic degree a graduate engineer
under the direction of

Univ.Prof. Dipl.-Ing. Dr.-Ing. Norbert Görtz

and

Dipl.-Ing. Martin Mayer

at the Institute of Telecommunications

submitted at Vienna University of Technology
Faculty of Electrical Engineering and Information Technology

by

Blanca Ramos Elbal

Vienna, July 2015

I hereby declare that this thesis is my original work and it has been written by me in its entirety. I have acknowledged all the sources of information which have been used in the thesis.

Blanca Ramos Elbal
Vienna, July 2015

Abstract

The Radio Frequency IDentification (RFID) technology has expanded rapidly and became very important during the last decades. New application are quickly emerging, as well as new protocols in order to reduce the identification process time.

The Wireless Identification and Sensing Platform (WISP) was developed by Joshua R. Smith et al. in order to investigate RFID combined with computing and sensing applications. The WISP is an open source, open architecture EPCglobal conform RFID tag, operating in the Ultra High Frequency (UHF) band. It comprises a fully programmable low power 16 bit microcontroller, sensors and an energy harvesting stage that enables passive operation, i.e., the WISP is completely supplied by the electromagnetic field emitted by an RFID reader. To transport information from WISP to reader, the WISP modulates its antenna load impedance according to the data, thereby producing an amplitude-modulated backscatter signal that is captured by the reader.

In this work, the properties of WISPs are investigated in order to determine their operational characteristics, implement new protocols and find out the characteristics of a multiple tag scenario. To that end, firmware for various application cases was written, radio frequency measurements were conducted and the results were evaluated. Through that course of action, some implementation obstacles were identified: considering several WISPs to be read out simultaneously, they have to be placed with a sufficient spacing, and synchronizing their responses remains a challenge.

Acknowledgments

I want to express my gratitude to Ing. B.Sc. Wolfgang Gartner for helping me, especially during the first days when I arrived to the university. I would like to thank Dipl.-Ing. Dr.techn. Robert Langwieser for his help, particularly on all aspects related to measuring equipment.

I owe my gratitude to my advisors Univ.Prof. Dipl.-Ing. Norbert Görtz, for giving me the opportunity to carry out this work, and especially Dipl.-Ing. Martin Mayer for his patience and all the help he granted me.

Thanks to all people from Vienna who helped me. Finally, I would like to thank my family because without them this experience would not have been possible.

Contents

Chapter 1.

Introduction

The Radio Frequency IDentification (RFID) technology was primarily developed during the Second World War and has been used for many years, not only for military purposes but also in civil applications. This technology consists of the wireless transfer of information in order to identify and track objects by using Radio Frequency (RF) transmission. In Figure 1.1 is illustrated a basic RFID system. In such system, the reader broadcasts a signal which is received by the tag. If the tag is charged with enough energy (passive operation), it sends back an identifying response. It should be pointed out that RFID systems are frequently multiple tag scenarios and they can be also multiple reader scenarios.

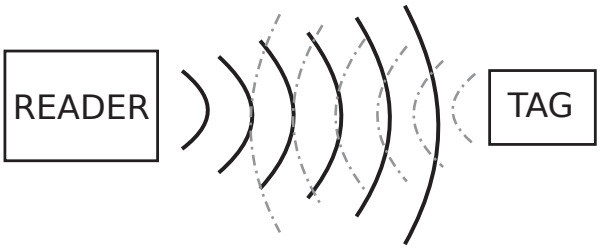

Figure 1.1.: Basic RFID system

Civil applications utilize RFID for tracking animals, access control, toll collection systems and contactless payment among others [1]. These applications can be either single tag scenarios or multiple tag scenarios. For example, RFID can be used in a supermarket for different purposes. If there is one reader in each shelf and each product has a tag attached, the inventory control could be done automatically. Furthermore, the customer could pass near a reader with the shopping trolley and the total price could be computed immediately.

In many applications, RFID has replaced barcoding. Indeed, barcoding works in a similar way as RFID. There is a label with information on it, and there is also a reader that gets the information from the label. In an RFID system instead of having a label with a barcode on it, there is a tag with an antenna and a microchip which stores information. This information is then transferred to a receiver which is sending signals and asking for the tag information. The most important advantages of RFID in contrast to barcoding are listed as follows:

- RFID is wireless: Line of sight is not needed like it is with barcoding.
- Stored information: A barcode cannot store as much information as an RFID tag. Apart from that, the information barcodes contain is fixed, and this is not always the case with an RFID tag.

1.1. Components of an RFID System

An RFID system is basically comprised of two parts: a reader and a transponder [2].

Reader

The interrogator or reader employs one or several antennas in order to communicate with the transponder. Depending on the antenna configuration, the RFID reader can be monostatic or bistatic [3]. Monostatic readers use the same antenna for either transmitting or receiving information. Conversely, bistatics readers use separate antennas for the communication with the tag. Therefore, a bistatic system has two separate RF channels.

Transponder

RFID transponders or tags are the data holders and are attached to the objects to be identified. As shown in Figure 1.2, most of them are basically made up of three parts [2] :

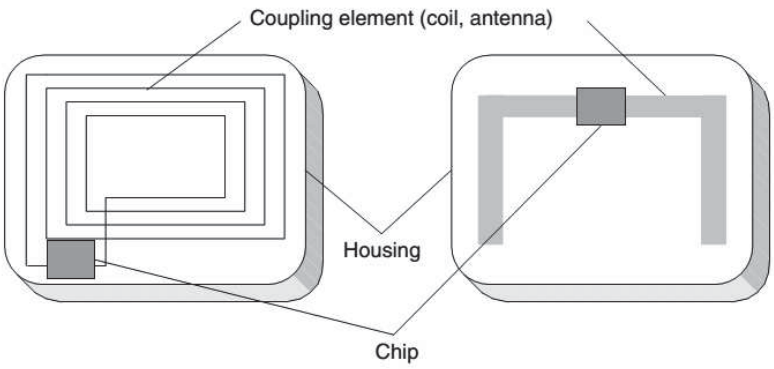

Figure 1.2.: Basic layout of a transponder

- **IC**: The integrated circuit is the brain of the tag, where the information is saved. One of the most important parts of it is the type and capacity of the memory. A larger memory will allow the transponder to store and, therefore, send a larger amount of data. However, there are also chip-less tags [4]. Such tags do not store an identification number.
- **Antenna**: The antenna determines things such as how far away the tag can send its data, how accurately it can send the data, and the operating frequency. Depending on the operating field the antenna will be a coil or a dipole.
- **Encasement**: Finally, the tag comprises a holder for the antenna and the chip, which can take many forms such as a card, a label, or a hard case.

When it comes to energy issues, RFID transponders can be classified into three categories:

- **Active**: They have their own battery source. Because of this, they can broadcast over a large range. Such battery is used to run the tag's microprocessor and to broadcast a signal to a reader.
- **Semi-passive**: They have an on-board power supply but, unlike active tags, they only use the battery to run the internal circuitry, and communicate by using the energy of the radio wave transmitted by the reader.

- **Passive**: These tags procure all of their energy to operate from the reader, so they have a much more limited read range. Such range goes from 10 cm (ISO 14443) to a few meters (EPC and ISO 18000-6) depending on the operating frequency and the antenna design [5].

In Table 1.1 is shown the relation between the type of tag and the operating frequency. It also illustrates the approximate read range, i.e., the maximal distance between reader and transponder at which a communication is possible [6].

Band	**LF**	**HF**	**UHF**	**Mircowave**
Frequency	<135 kHz	13.56 MHz	850 to 950 MHz	2.4 to 2.45 GHz
Tag characteristics	Passive		Active, passive, semi-passive	Active, passive
Approximate read range (passive tags) (m)	2	0.1-0.2	4-7	1
Communication principle	Inductively-coupled systems		Electromagnetically-coupled systems	
Operating field	Near field		Far field, near field	Far field

Table 1.1.: Operating frequencies of different RFID systems

1.2. Principle of Operation

The communication between reader and tag can be established through magnetic or electromagnetic coupling [6], depending on the field of operation. Table 1.1 shows the frequency ranges and the operating principle for different RFID systems. The tag to reader communication (uplink) in near field arises from an amplitude modulation of the magnetic field emitted by a reader. On the other hand, the uplink communication in far field is the result of an amplitude modulation of the electromagnetic field from the reader that is reflected at the tag. That is to say, through backscatter modulation. As shown in Figure 1.3 [7], the reader transmit antenna sends out an RF signal to the tag. On the right side, the potential difference developed at the antenna energizes and powers up the tag. When the tag is charged with enough energy, it is able to respond to a query command issued by the reader. Such response is sent by varying the amplitude of the electromagnetic wave reflected by the tag according to the data to be transmitted. Such amplitude modulation is accomplished by switching the antenna load impedance between two states. It should be mentioned that in this example the reader is bistatic, and a direct path between both readers antennas is also depicted.

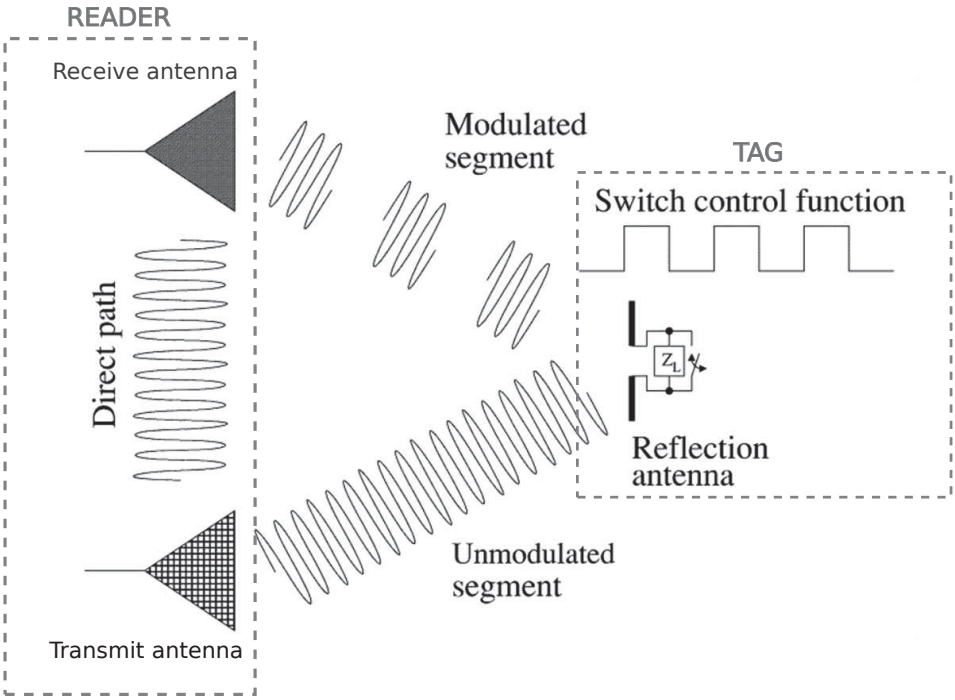

Figure 1.3.: Backscatter system

1.3. Wireless Sensor System Devices

In most commercial RFID systems, tags are fixed-function devices compliant with a specific protocol implemented on the tag with no chance of modifying it, nor the data replied by the tag. But nowadays, new platforms have been developed to extend the functionality of traditional tags. These additional features allow new experimentation options such as non-standard protocols. In Table 1.2 are shown several devices which play the role of a tag in an RFID system. They are re-programmable tags and there are some full or partial implementations available of several protocols used in RFID.

Platform	**WISP**	**TU Graz**		**Identec I-Q310**
Technology	Passive RFID (UHF)	Semi- Passive RFID (UHF)	Semi- Passive RFID (HF)	Active RFID
Protocol	EPC Gen2	ISO 18000-6C / EPC Gen2	ISO 15693 / ISO 18000-3 / NFC / ISO 14443A	ISO18000-7
Maximum read range (m)	3	15		100
Lifetime	Unlimited	Battery life cycle		Battery life cycle
Extensibility	Open Platform	Limited		No

Table 1.2.: Wireless sensor system devices

One of these platform is designed by the Institute of Applied Information Processing and Communications of Graz University of Technology. The TU Graz tag has two prototypes [8], one for High Frequency (HF) and another one used in UHF. Both of them have been developed on a Field-Programmable Gate Array (FPGA), which enables the tag to interact easily with additional devices, since they provide Serial Peripheral Interface (SPI), RS232 and

JTAG interfaces. Besides that, it has been designed to improve the security in RFID systems, so it entails high-speed processing. As a consequence, it has a high power consumption. These tags are semi-passive, which means that they have an on-board power source. But the potential customization of such tags is limited since the schematic or some digital sections are not provided.

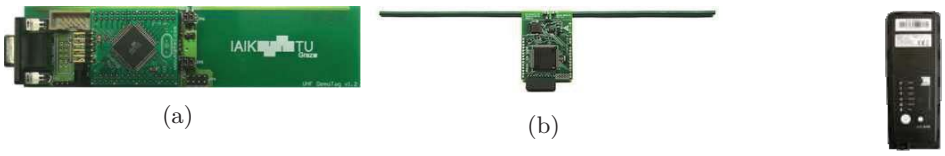

(a) (b) (c)

Figure 1.4.: Demo tag TU Graz (UHF), Moo platform, I-Q310 Sensor Transponder

On the other hand, there are also active tags, such as the Identec I-Q310 [9]. It has the largest read range and consumes between 17 and 20 mA [10]. In this case, the user does not have full access to the source code. It includes an on-board memory, user interface (LED) and a variety of internal sensors.

An example of passive wireless sensor system devices is the Wireless Identification and Sensing Platform (WISP) [11, 12], which is explained in detail in Chapter 2. This platform is totally open source, and design details such as schematics and layout are publicly available, as well as the source code. This triggered the development of the Moo platform [13]. The Moo 1.0 derives from the WISP 4.1. The changes performed to develop the Moo are focused on extending the capabilities of the WISP. The main hardware differences between both platforms are shown in Table 1.3. The Moo has a different microprocessor with differences between its Random-Access Memory (RAM) and Flash memories. The WISP comes with an on-chip Electrically Erasable Programmable Read-Only Memory (EEPROM). On the other hand, on the Moo platform such memory is replaced by a Flash memory which besides being faster is more capacious. As disadvantage, the power consumption is higher. The communication between the EEPROM memory and the microprocessor on the WISP is limited by the speed of the EEPROM memory to 100 kHz, while the microprocessor clock frequency can range up to 16 MHz. The on-chip flash memory of the Moo can work up to 40 MHz. Regarding the compatibility with readers and therefore the software implementation of the Electronic Product Code (EPC) Class 1 Gen 2 protocol [14], the Moo not only works with the "Impinj Speedway®" reader as does the WISP, but also supports "ThingMagic Mercury 5/5e®" readers.

1.4. Motivation of this Work

Nowadays a wide range of RFID applications require multiple tag scenarios, and many theoretical papers that focus on fast tag identification have been written. But such papers make unverified assumptions, for instance, that there are many tags in read range and that there is no mutual influence between them, regardless of the distance between the tags. Another important issue is the development of non standard protocols to improve the performance of Framed Slotted Aloha (FSA) [6]. For example, some approaches modify the FSA protocol by introducing orthogonal sequences into the tag response in order to acknowledge more than one tag per slot [15]. Other approaches utilize Code Division Multiple Access (CDMA) based protocols [16, 17], and recent works suggest compressed sensing based approaches [18, 19]. In

Feature	Moo	WISP 4.1
Microcontroller	MSP430F2618	MSP430F2618
RAM	8 kB	512 B
Flash memory	16 kB	8 kB
Power Consumption (1 MHz, 2.2V)	365 μA	250 μA
On chip-memory	Flash	EEPROM
Memory size	4 Mb	1 Mb
Clock frequency	40 MHz	100 kHz
Standby current	2 μA	100 nA

Table 1.3.: Moo and WISP hardware differences

these theoretical works, it is frequently taken for granted that all tag responses are perfectly synchronized and they have the same link frequency.

In order to investigate the reliability of these assumptions, the WISP is used since it is a fully-programmable device that could potentially be used to implement and test such new schemes.

1.5. Outline

This work is structured as follows. Chapter 2 presents the WISP in more detail. In Chapter 3 some measurements are carried out in order to characterize both the behavior of one single WISP and the possible influence between several WISPs. Chapter 4 deals with the synchronization between tags and therefore the internal differences between several WISPs. In Chapter 5 is performed the channel estimation with one single WISP as well as the channel estimation with two WISPs. Lastly, Chapter 6 presents the conclusions reached as a result of this work.

Chapter 2.

Wireless Identification and Sensing Platform

2.1. Introduction

The Wireless Identification and Sensing Platform (WISP) [11, 20] is a sensing and computing device completely supplied by the electromagnetic field emitted by an RFID reader. This means that it has the role of a passive tag in an RFID system. The WISP was developed by Intel for the purpose of combining RFID systems and sensor networks [21]. In other words, to develop a passive tag which could also be a sensor. This approach would eliminate batteries and get rid of the power problem in sensor networks. In this way, creating a system which retains the sensing and computing capabilities of wireless sensor networks but also keeping the simplicity of an RFID system. For example, sensor network are usually multi-hop networks but RFID systems are not.

The first prototype was the α-WISP [22] illustrated by Figure 2.1. In such platform, there were two integrated circuits, each one with a different identification number and just one antenna. Depending on the inclination, the tag would send back a different identification to the reader [23]. Therefore the α-WISP was a one bit accelerometer sensor.

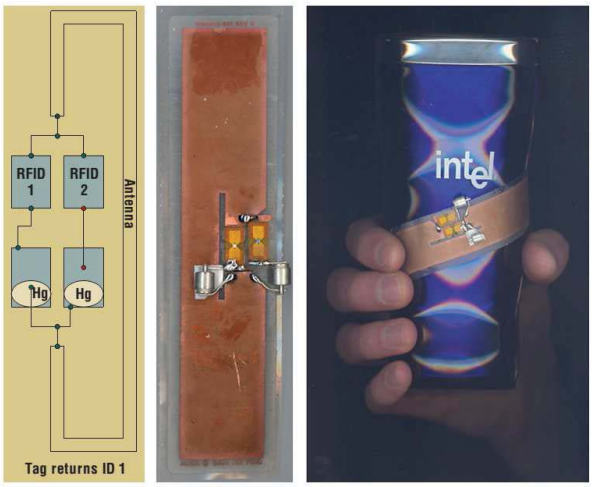

Figure 2.1.: α-WISP

After the α-WISP, the π-WISP was developed with the aim of sending more than one bit of sensor data. These first two prototypes encoded sensor information by toggling several commercial RFID Integrated Circuits (ICs). In order to control completely the information transmitted by the tag, a new tag design was developed without using commercial RFID ICs. Thus was developed the general purpose Wireless Identification and Sensing Platform (WISP) according to the EPC Class 1 Generation 1 protocol. Unlike previous prototypes, the WISP

encodes the sensor data in special bits reserved in the protocol. Later on, the EPC Class 1 Generation 1 protocol was replaced by the EPC Class 1 Generation 2 protocol [14].

The platform used in this work is the WISP 4.1[1] illustrated by Figure 2.2. The WISP has several sensors like a 3-axis accelerometer, temperature sensor, analog voltage sensor and a capacitance sensor.

Figure 2.2.: Wireless Identification and Sensing Platform (WISP) 4.1

2.2. Hardware Architecture

The WISP includes an on-board fully programmable low power 16 bit Texas Instruments MSP430F2132 microcontroller. The most important characteristics of such microcontroller family are summarized in Table 2.1 [24, 25].

Supply Voltage Range	1.8-3.6 V
Power Consumption	Active Mode: 250 μA at 1 MHz, 2.2 V Standby Mode: 0.7 μA Off Mode (RAM Retention): 0.1 μA
Architecture	16 bit RISC[2]
Flash Memory	8 kB
RAM	512 B

Table 2.1.: MSP430F21x2 microcontroller characteristics

MSP430 Basic Clock Module

The microcontroller counts on several clock sources:

- **Internal Very-Low-Power Low-Frequency Oscillator (VLO)**: Supports a typical frequency of 12 kHz without using a crystal.
- **LFXT1 oscillator**: Enables ultra low current consumption using a 32.768 kHz watch crystal oscillator in Low Frequency (LF) mode and it also supports high-speed crystals in HF mode.

[1] Named just as WISP hereinafter.
[2] Reduced Instruction Set Computer.

- **Digitally Controlled Oscillator (DCO)**: Its frequency range goes from 0.06 MHz to 26 MHz. It can be adjusted by software through the values of DCOx and RSELx. But, as shown in Figure 2.3, it cannot be set to a particular frequency but only to a frequency range since the DCO has a certain deviation.

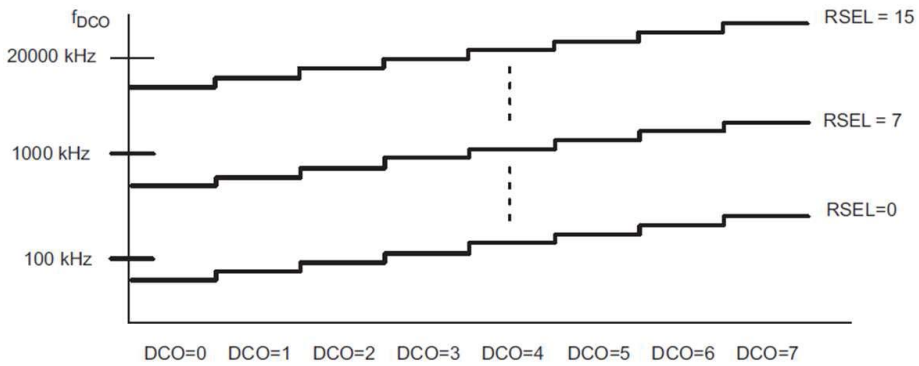

Figure 2.3.: Typical DCO range and RSEL steps [25]

On the standard firmware compliant to EPC protocol that is available, the VLO is not used. There are three clock signals available: Main clock (MCLK) used by the CPU, Sub-Main clock (SMCLK) and Auxiliary clock (ACLK), both used by peripherals. It also offers support for five Low Power Modes (LPMs). The difference between the Active Mode (AM) and the LPMs lies in the clock sources that are activated. Such relation is shown in Table 2.2.

Mode	CPU and Clocks Status
Active	CPU is active, all enabled clocks are active
LPM0	CPU, MCLK are disabled, SMCLK, ACLK are active
LPM1	CPU, MCLK are disabled. DCO and DC generator are disabled if the DCO is not used for SMCLK. ACLK is active
LPM2	CPU, MCLK, SMCLK, DCO are disabled. DC generator remains enabled. ACLK is active.
LPM3	CPU, MCLK, SMCLK, DCO are disabled. DC generator disabled. ACLK is active.
LPM4	CPU and all clocks disabled

Table 2.2.: Operating modes for Basic Clock System

WISP Block Diagram

In Figure 2.4 the WISP block diagram is depicted [20]. First of all, the RF signal from the reader is received at the dipole antenna and passes through the impedance matching network that is intended to match the antenna to the analog front end. Since the WISP is a

passive platform, it contains a power harvester module to provide the power supply instead of a battery. The voltage regulator provides a constant voltage to the microcontroller. As shown in Table 2.1, the lowest voltage to operate is 1.8 V. This voltage entails the lowest power consumption. The demodulator extracts data from the incoming signal from the reader. Moreover, the external sensors are powered up and measured by the microcontroller (MCU). The uplink data are sent through the modulator, which backscatters information to the reader.

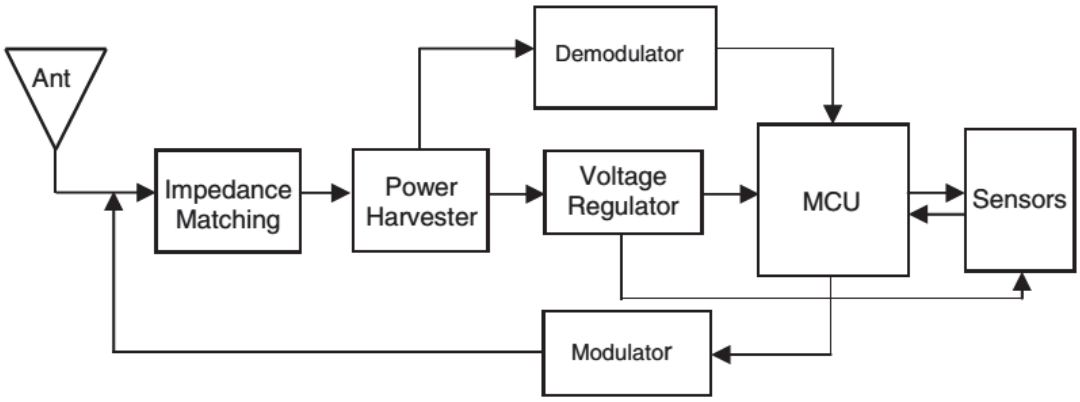

Figure 2.4.: WISP block diagram

2.3. Software

Implemented protocol

The firmware available [11] implements partially the EPC Class 1 Generation 2 standard. Some states like *secured* and *killed* are not implemented, as well as commands like *write*, *kill*, *lock* or *access*. Furthermore, the firmware available does not support FM0 modulation, just Miller modulation.

Power management algorithm

Passive RFID tags have stringent low-power requirements, hence they should consume on average as little power as possible. This is achieved by duty cycling between the AM and the Low Power Mode 4 (LPM4). The power management algorithm is depicted in Figure 2.5. Initially the WISP is powered down and far away from the reader. When the WISP enters into the reader's range it begins to harvest power. When the voltage stored is enough for operation the WISP powers up in a reset state and it begins to execute code. The WISP generates the packet that later on will be sent to the reader. At this point are performed tasks such as calculate the CRC or the sensor measurement. Immediately after that, the WISP goes to the LPM4 to avoid running out of energy and therefore to suffer a hard reset. When the WISP receives the query of the reader, it enters again the AM and sends back an appropriate response.

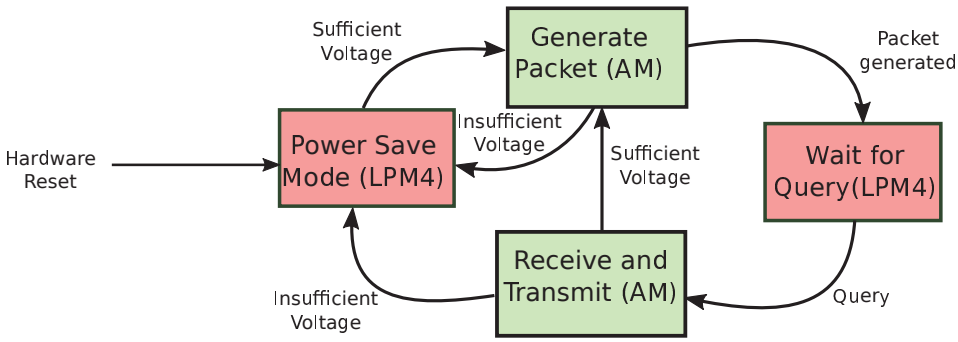

Figure 2.5.: Operational power cycle

2.4. New WISP

A new generation of WISPs has been developed. The WISP 5 has two versions: WISP 5.0 LRG for long-range operation, and WISP 5.0 HPW for more efficient operation at short range [26].

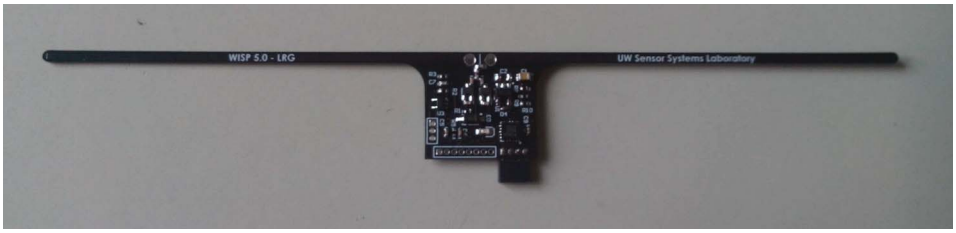

Figure 2.6.: WISP version 5.0

The most significant new features with respect to the previous version are that the WISP 5 supports FM0 encoding, the firmware available as open source implements *read* and *write* commands, and a different microcontroller is used. The WISP 5 has an MSP430FR5969 microcontroller with FRAM (Ferroelectric RAM) memory. The advantages of this kind of memory over the FLASH memory of the WISP 4.1 are a higher write speed, a higher write endurance and a lower power consumption. Note that such memories are inside the microcontrollers, they are not on-board memories. As explained in section 1.3, the WISP 4.1 has an EEPROM as a external memory.

Although the new version is already available and a initial characterization was carried out, it is not used in the thesis due to the problems of the rectifier stage design. In order to illustrate such problem, Figure 2.7 shows the rectified voltage of the WISP 5 in LPM4 with a constant power transmitted by the reader P_{TX} and a fixed distance from the reader D, for several values of P_{TX}. The setup used to take the measurements is explained in section 3.1. The problem encountered in the WISP 5 is that its rectified voltage breaks down periodically and triggers the reset, while the WISP 4.1 delivers a constant rectified voltage.

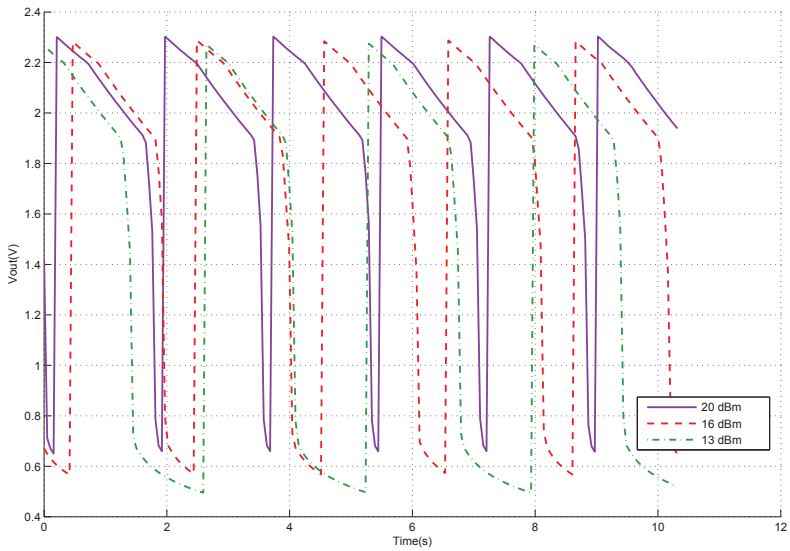

Figure 2.7.: Time sweep of the rectified voltage in WISP 5 ($D = 70\,\text{cm},\ f = 862\,\text{MHz},\ P_{TX} = \{13\,, 16\,, 20\}\,\text{dBm}$)

Chapter 3.

Operating Characteristics

In this chapter are presented the results obtained from the measurements carried out. The purpose of these measurements is to characterize the WISP, and to determine the differences that may exist between WISPs as well as the mutual influence among WISPs. It should be mentioned that the three platforms available are numerated as WISP 461, WISP 462 and WISP 463, but for the remainder of this work they will be named as WISP 1, WISP 2 and WISP 3, respectively.

3.1. Measurement Setup

The measurements carried out in the present chapter were performed with the setup illustrated by Figure 3.1. The reader is emulated by signal generator SMU 200A [27]. The transmit antenna of the reader is a micro strip patch antenna with a resonant frequency of 868 MHz and a gain of 7.1dBi [28]. For these measurements just a carrier wave without modulation will be sent since only transmit capabilities are required in this chapter. The rectified voltage of the WISP, *Vout*, will be measured with a digital multimeter [29]. Such voltage is measured between the power harvester block and the voltage regulator in Figure 2.4. Furthermore, the WISP is separated from the reader by a distance D.

3.2. Firmware Changes

In order to characterize the behavior of the WISP, the EPC Class 1 Generation 2 protocol compliant firmware available is not used, since the duty cycling could cause an outcome difficult to interpret. Instead, a custom firmware is used. When a sufficient amount of energy is harvested and the WISP wakes up, it enters an idle state. The WISP is programed to be either in the Active Mode (AM), or in a Low Power Mode (LPM) where some clock sources are deactivated, see Table 2.2.

3.3. Antenna Matching

3.3.1. Single WISP

The first step to performance any measurement is to determine the appropriate operating frequency. So as to find it out, a frequency sweep is carried out in both AM and LPM. The results are plotted in Figure 3.2. When the WISP is in AM, the matching point is around 862.5 MHz while in the LPM4 it is slightly higher.

It can be concluded that there is no difference in the matching point of the antenna between different devices. On the other hand, the rectified voltage differs, but as shown in Figure 3.1, the WISP was not attached to any rigid support. For this reason, the orientation may change and therefore the rectified voltage.

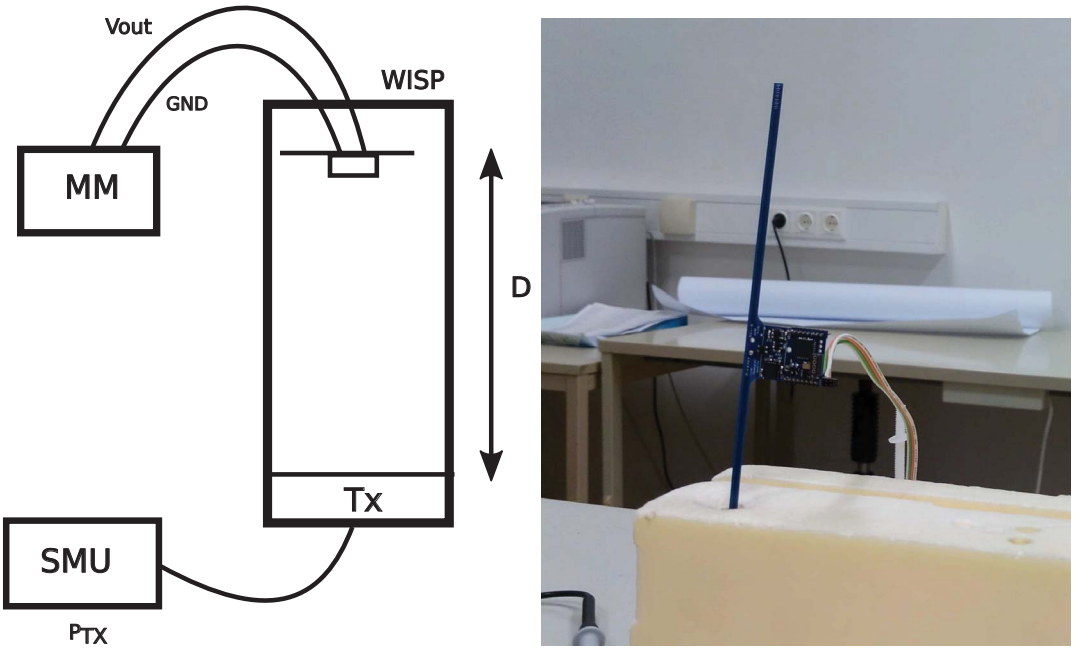

(a) (b)

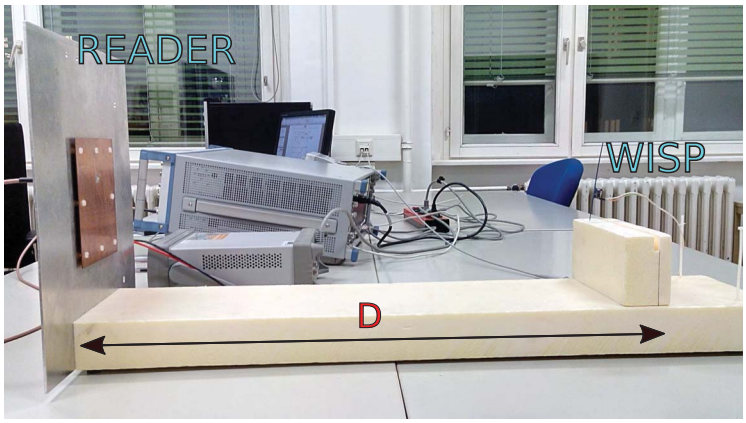

(c)

Figure 3.1.: Setup 1: WISP characterization

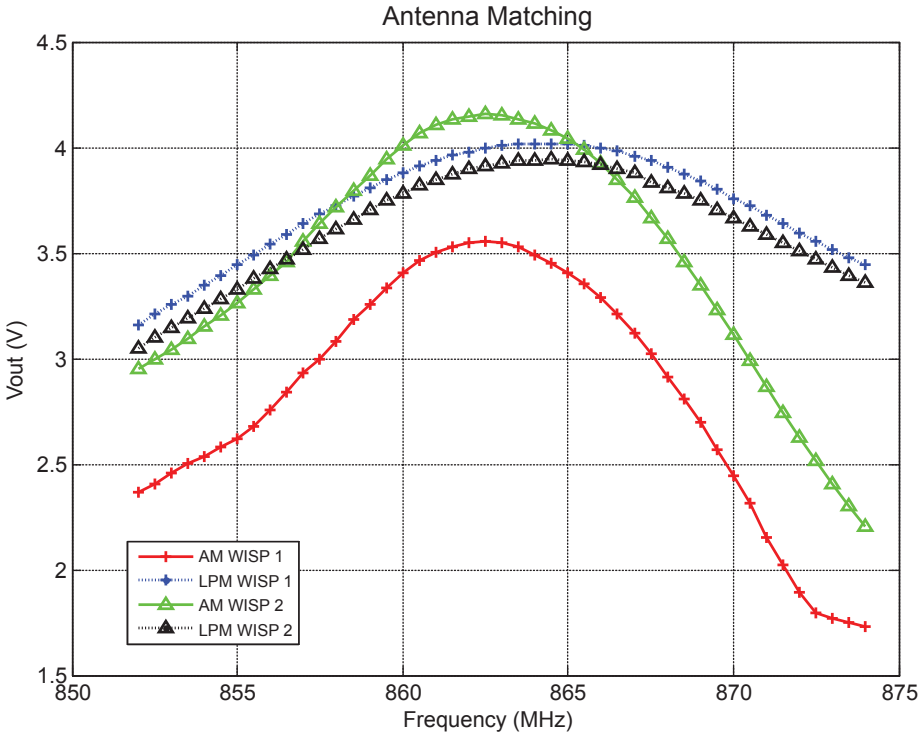

Figure 3.2.: Frequency sweep in AM and LPM4 with two WISPs individually ($P_{TX} = 25\,\text{dBm}, D = 50\,\text{cm}$)

3.3.2. Multiple WISPs

With a view to have a multiple tag scenario, two WISPs are placed with a distance from the reader D, and a distance d between them, as shown is Figure 3.3. This time, the platforms are attached to a rigid support to observe the differences in the rectified voltage *Vout*.

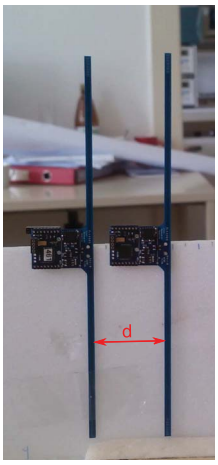

Figure 3.3.: Placing of WISPs to measure the mutual influence

The results are plotted in Figure 3.4. It can be concluded that with the considered set of distances, the mutual influence between WISPs does not cause big changes in the matching point, but it strongly affects the rectified voltage.

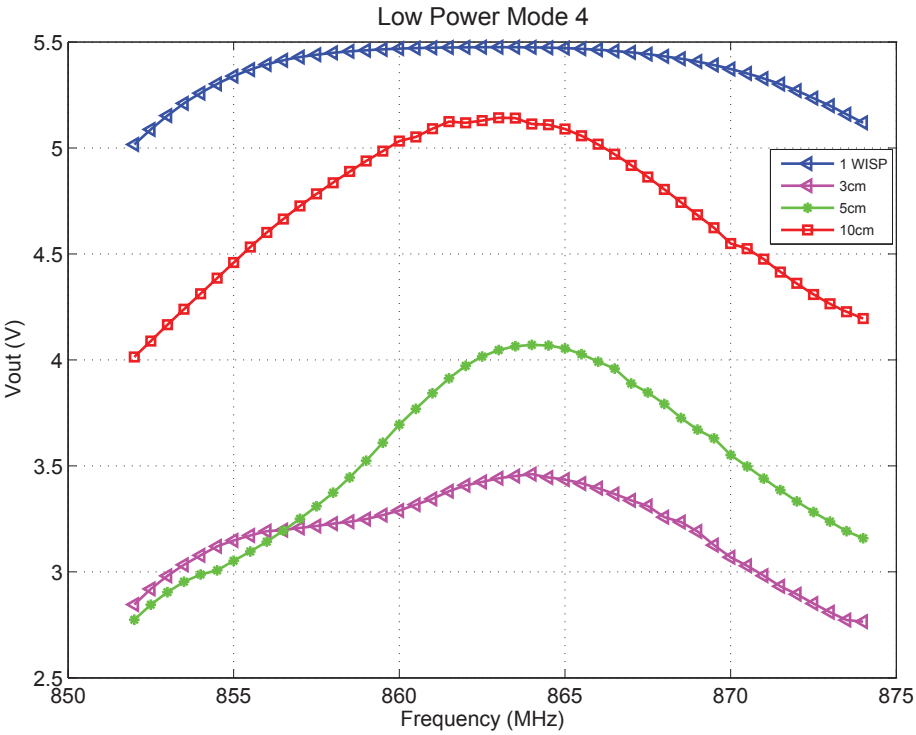

Figure 3.4.: Frequency sweep in LPM4 with one single WISP and two WISPs separated by a distance of $d = \{3\,,5\,,10\}$ cm ($P_{TX} = 19\,\text{dBm}, D = 50\,\text{cm}$)

Three WISPs

Now three WISPs are placed close to each other and the rectified voltage is measured in the middle platform, as shown in Figure 3.5. As mentioned above, the mutual influence between two WISPs separated by $d = 10\,\text{cm}$ is small, but with three WISPs the matching point is displaced by approximately 5 MHz upwards.

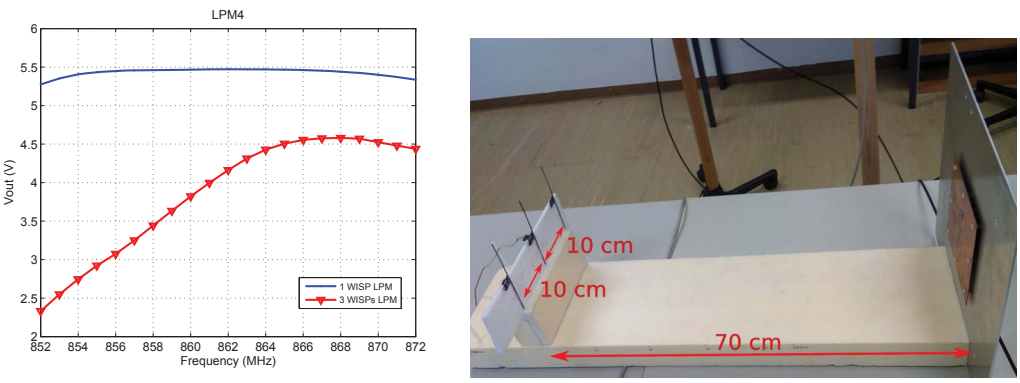

(a) (b)

Figure 3.5.: Frequency sweep in LPM4 with tree WISPs separated by a distance of $d = 10\,\text{cm}$ between them and a distance of $D = 70\,\text{cm}$ from the reader

3.4. Verification of Measurement Setup

In Setup 1 illustrated by Figure 3.1, the ground of the WISP is connected to the multimeter ground. Since one of the ports of the antenna dipole is directly connected to the WISP ground, the influence of the multimeter may change the matching point of the antenna. To ensure the reliability of such setup, the multimeter is replaced by an oscilloscope and the potential difference between two probes is measured in order to emulate a differential probe. The same measures are done with the oscilloscope and the multimeter. The results are shown in Figure 3.6. In view of the results obtained, it can be concluded that the multimeter does not influence the antenna matching point notably and therefore Setup 1 is acceptable to do measurements.

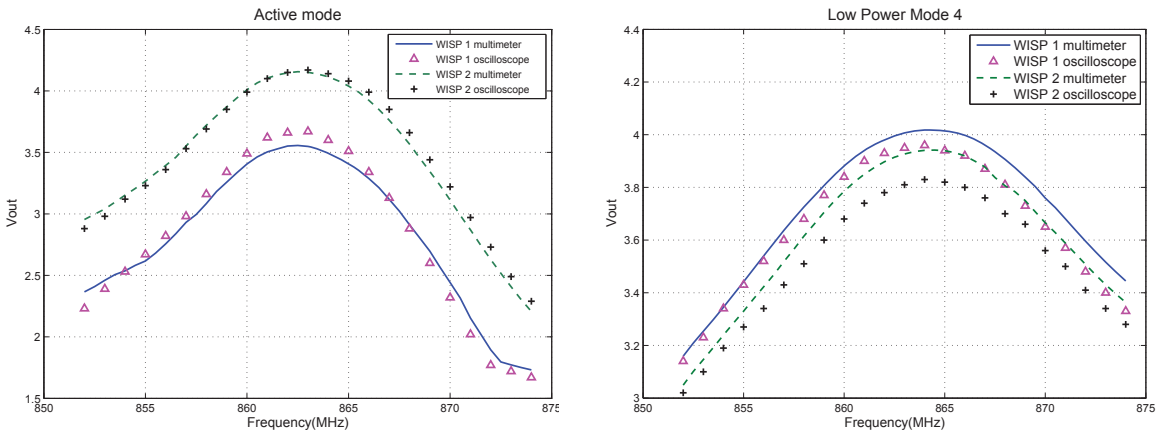

(a) (b)

Figure 3.6.: Verification of the multimeter influence

3.5. Power Consumption and Power Up Process

3.5.1. Single WISP

As explained in section 2.2, the microprocessor needs at least 1.8 V of rectified voltage to power up. In order to find out the relation between the transmit power P_{TX} (controlled at SMU) and the distance necessary to operate, a power sweep is carried out with a fixed distance from the reader D. In Figure 3.7 the AM and the different LPMs are plotted. Since the WISP performs a duty cycling between the AM and the LPM4 in the standard compliant firmware, the average consumption while it is in operation will be between these curves.

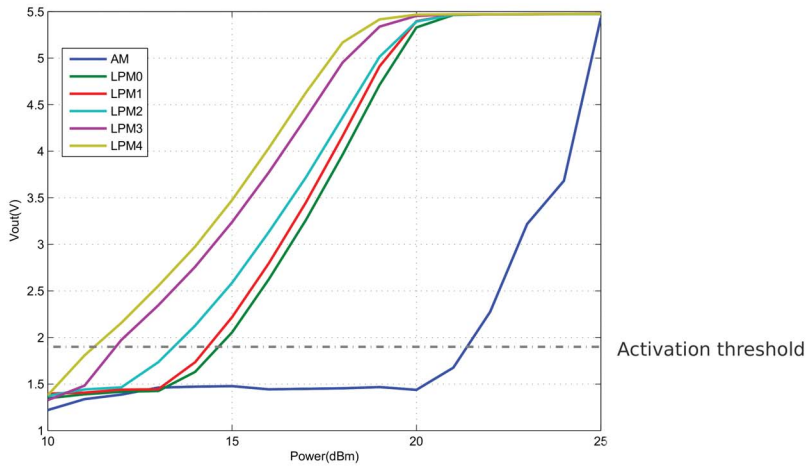

Figure 3.7.: Power up process in AM and the different LPMs ($f = 862\,\text{MHz}, D = 70\,\text{cm}$)

3.5.2. Multiple WISPs

As mentioned above, the influence of other platforms does not have a huge effect on the antenna matching point, but it has on the rectified voltage. Figure 3.8 illustrates the rectified voltage related to the transmitted power by the reader when the WISP is influenced by other tags.

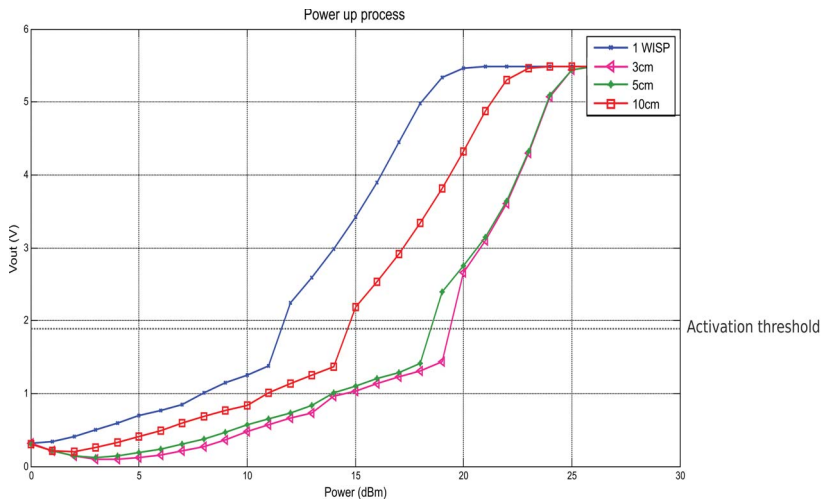

Figure 3.8.: Power up process in LPM4 with one single WISP and two WISPs separated by $d = \{3, 5, 10\}\,\text{cm}$ ($f = 863\,\text{MHz}, D = 50\,\text{cm}$)

It can be concluded that the proximity of other platforms causes a huge difference in the rectified voltage. When two WISPs are close ($d = 3\,\text{cm}$), around 8 dB more are required in comparison to the transmitted power necessary to wake up one single WISP.

3.5.3. Capacitor Discharge

In Figure 3.9 can be observed the WISP behavior over the time with a fixed distance from the reader D, carrier frequency f and variable transmit power $\mathrm{P_{TX}}$. At first the carrier is off. Then it is turned on for some time and then turned off. The capacitors of the rectifier

stage hold some charge that is depleted faster in the active mode, therefore the voltage breaks down faster. In other words, the AM drains more current than the LPM4, which confirms that without the duty cycling the WISP could easily suffer a hard reset.

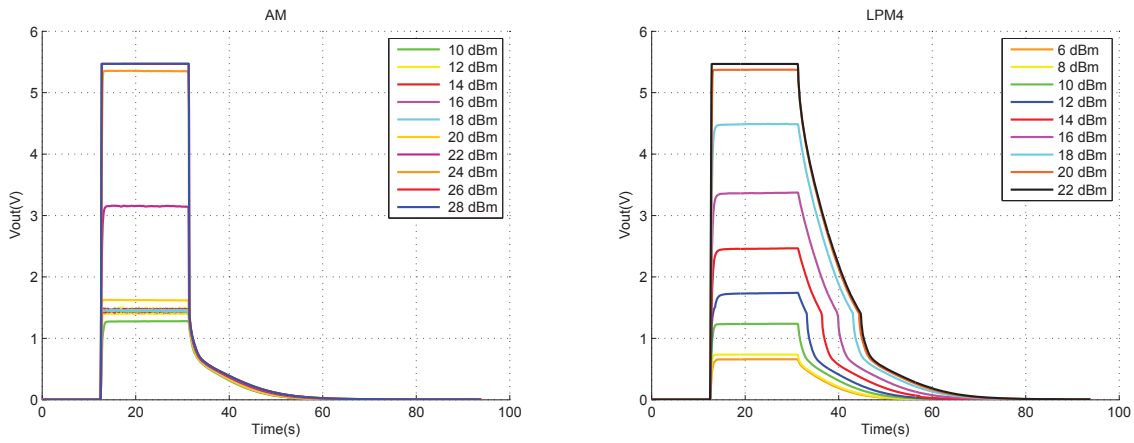

(a) (b)

Figure 3.9.: Rectified voltage *Vout* of the WISP over the time at variable P_{TX} ($D = 70\,\text{cm},\ f = 862\,\text{MHz}$)

Chapter 4.

Timing and Clock Fidelity

This chapter describes the process and results of the comparison between the clock of different WISPs. Such comparison will be carried out by measuring the jitter, that is to say, the deviation of the clock signal and consequently the change of the pulse width over the time, as well as the time to respond of the WISPs.

4.1. Measurement Setup

The measurement setup is illustrated by Figure 4.1. The reader is composed of a signal generator [27] connected to the transmit antenna and a signal analyzer [30] connected to the receive antenna. The WISP is separated from the reader by a fixed distance of $D = 60\,\text{cm}$, the carrier power and frequency are $\text{P}_{\text{TX}} = 25$ dBm and $f = 862$ MHz, respectively.

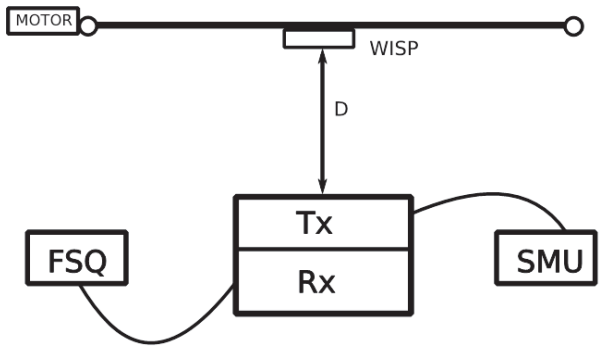

Figure 4.1.: Setup 2: Clock fidelity

In Figure 4.2 is depicted the FSQ block diagram [30]. For the measurements, the resolution bandwidth (RBW), i.e., the bandwidth of the analog filters in front of the A/D converter, is set to 2 MHz. Since the RBW is up to 100 kHz, the FSQ uses digital bandpass filters with a Gaussian shape. The output sampling rate can be set between 10 kHz and 81.6 MHz, and for these measurements it is 10 MHz. The acquisition time is 0.9 ms, consequently 9000 samples are taken.

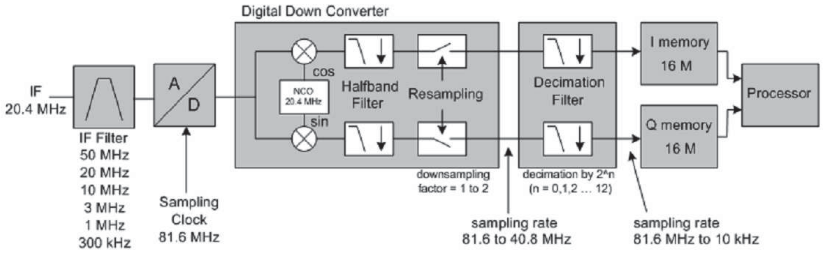

Figure 4.2.: Block diagram illustrating the FSQ signal processing

4.2. Firmware Changes

In order to measure the initial delay[1] and the jitter, the available firmware is modified in order to create the response shown in Figure 4.3. Such response consists of 1028 bits, by understanding bit as a '0' or a '1'.

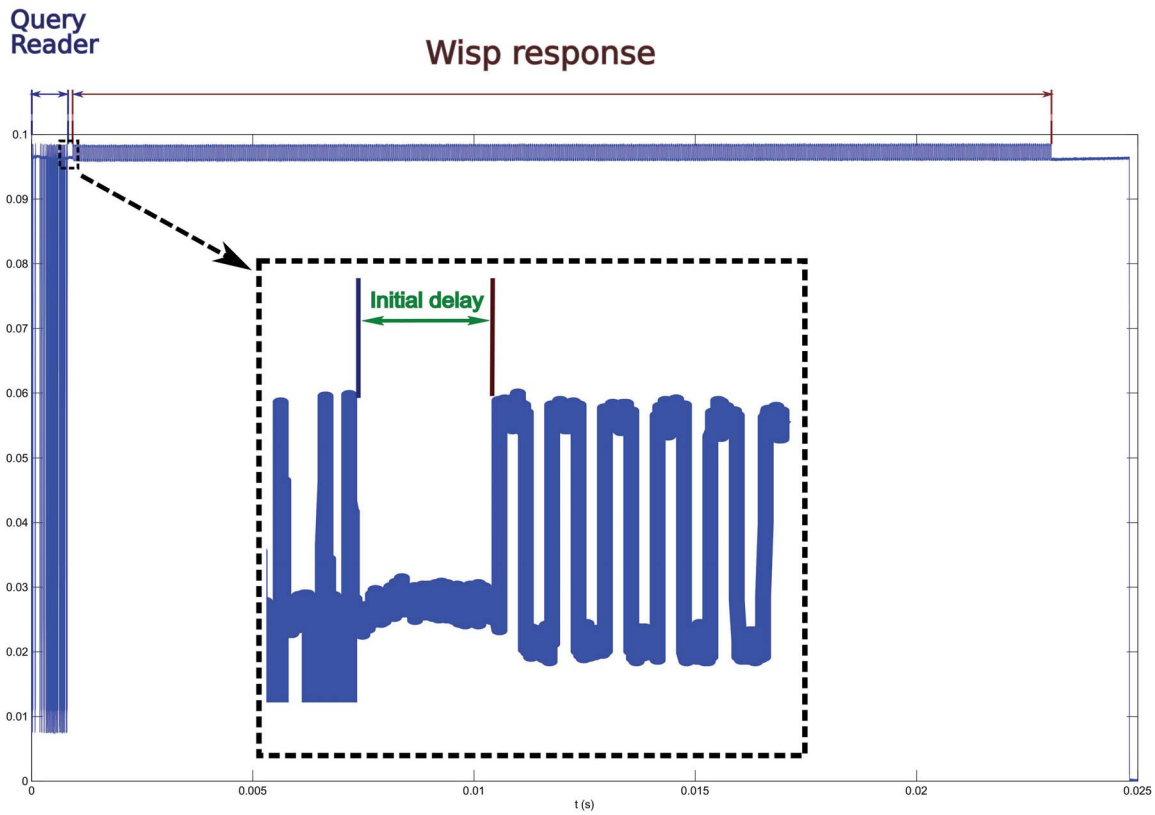

Figure 4.3.: Query reader and custom WISP response to estimate the delay and jitter

[1]Time between interrogator transmission to tag response

4.3. Delay Measurement

In order to find out the deviation between the different DCOs, the same firmware is loaded in the three WISPs. Over the time 200 repetitions are taken and the initial delay is measured. The result is plotted in Figure 4.4. Here, the first problem of channel estimation with CDMA techniques becomes apparent. Though the same DCO range frequency is selected, the deviation of the different clocks is very relevant. The outliers may be due to the modification of the firmware. In such modification, the WISP counts bits of the query sent by the reader. If the WISP does not recognize some bit, the time to reach the total number of bits would be longer and therefore the WISP time to respond will be longer. These outliers might seem very deviated from the mean, but in none of the cases are bigger than the pulse width.

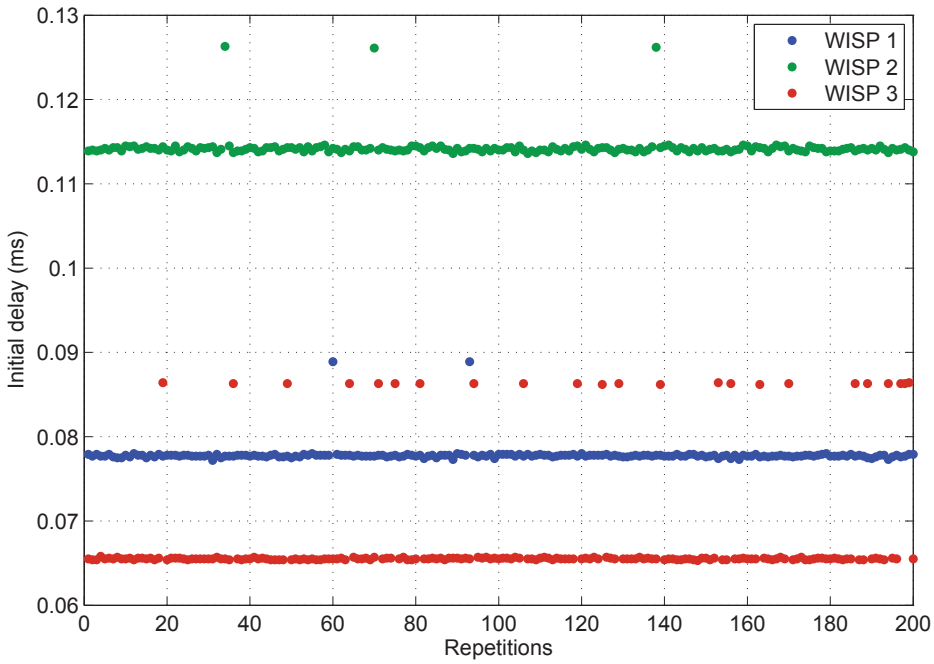

Figure 4.4.: Initial delay measurement

Initial delay in commercial tags

In order to compare the WISP to a commercial tag, the same measurement is carried out with both tags. In this case, the WISP uses the available firmware that is compliant to the EPC protocol. The commercial tag used in this comparison is the UBIK-808 UHF tag, shown in Figure 4.5. It supports both ISO-18000 6C protocol and EPC Class 1 Gen 2 protocol [31].

Figure 4.5.: Commercial tag used in the comparison

The measurements are executed for a fixed frequency and transmitted power on the reader, and for two different distances between tag and reader, $D = \{60, 90\}$ cm. The results are presented in Figure 4.6. It should be mentioned that when the WISP replies with a long sequence, such sequence does not fade when it is far away from the reader. Note that this comparison is made with the WISP 1, but if the initial delay of the commercial tag is compared with the initial delay of the other WISPs shown in Figure 4.4, it is just 2 ms bigger than the initial delay of the WISP 2. The WISP is not responding all the time. This may be because the WISP does not recognize all bits of the query from the reader. This fact is not related with the distance since the response probabilities are $P_{60\text{ cm}} = 0.820$, $P_{90\text{ cm}} = 0.825$. Though for these measurements the probability of response at $D = 90$ cm is higher, it should be noted that the difference to the case of $D = 60$ cm is just one sample.

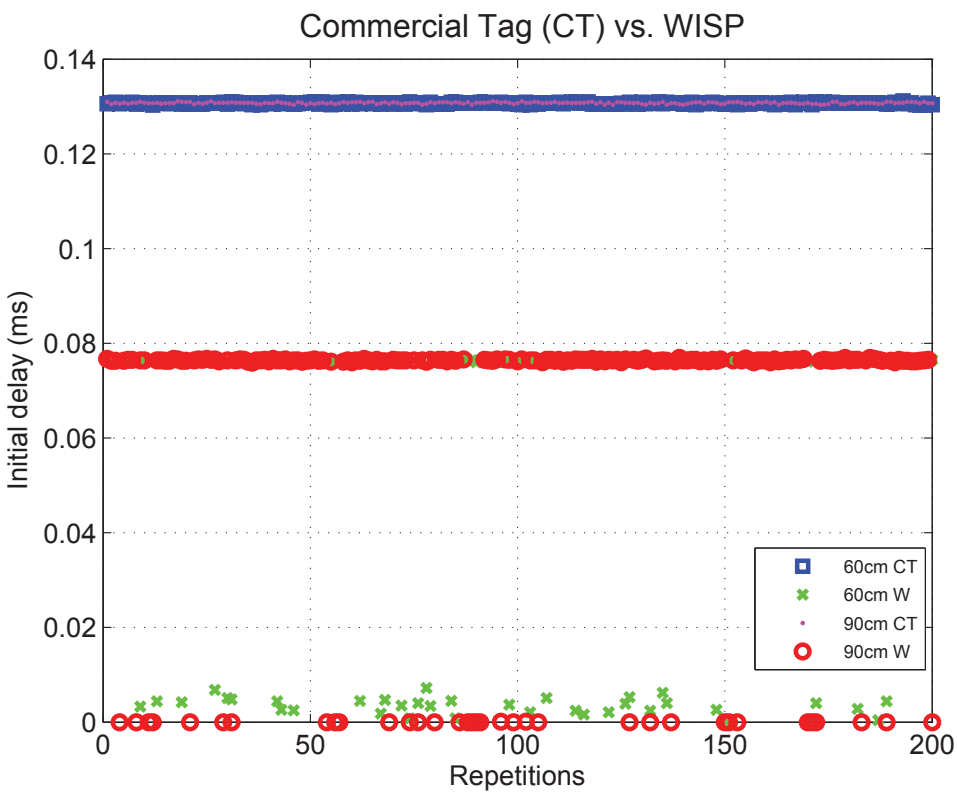

Figure 4.6.: Initial delay of WISP 1 and a commercial tag ($P_{TX} = 25$ dBm, $f = 862$ MHz)

4.4. Jitter Measurement

Using a single response as shown in Figure 4.3, the width of each bit is measured. Since there are 1028 bits (Figure 4.7), the mean pulse width can be calculated as $\bar{t}_p = \frac{T_p}{1028}$.

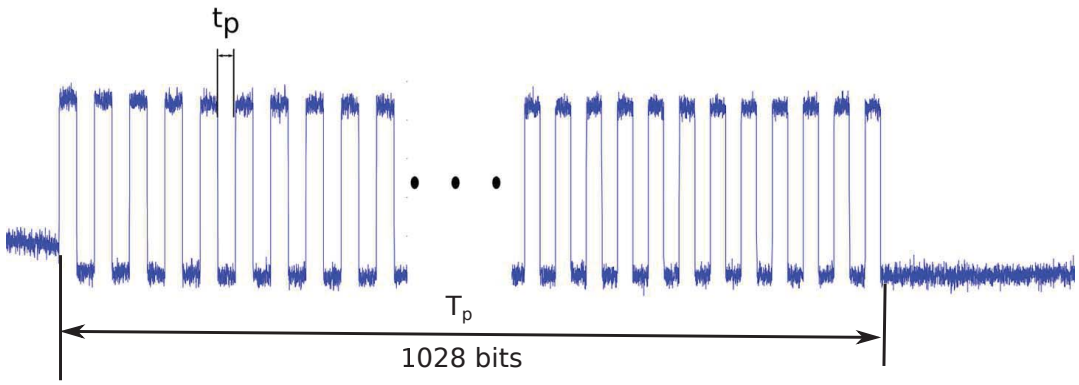

Figure 4.7.: Jitter estimation

The results of the mean pulse width and the standard deviation for each WISP are shown in Table 4.1. Since the standard deviation σ_p is very small in all cases, it can be concluded that the DCO does not change its behavior over the time. On the other hand, the DCOs of the different WISPs run at different frequencies.

	WISP 1	**WISP 2**	**WISP 3**
Pulse width mean	$\overline{t_{p1}} = 19.47\mu s$	$\overline{t_{p2}} = 21.49\mu s$	$\overline{t_{p3}} = 18.52\mu s$
Pulse width standard deviation	$\sigma_{p1} = 2.81\mu s$	$\sigma_{p2} = 4.93\mu s$	$\sigma_{p3} = 1.38\mu s$
Initial delay mean	$\overline{t_{i1}} = 0.0778\,\mathrm{ms}$	$\overline{t_{i2}} = 0.1143\,\mathrm{ms}$	$\overline{t_{i3}} = 0.0679\,\mathrm{ms}$

Table 4.1.: Pulse width mean, pulse width standard deviation and initial delay mean for the three different WISPs

Chapter 5.

Channel Estimation

In this chapter the channel coefficient is measured with one single WISP in section 5.5 and with two WISPs utilizing Code Division Multiple Access (CDMA) in section 5.6. Since the EPC protocol does not feature sequences for channel estimation with several WISPs, the firmware has to be adapted in order to perform channel estimation with orthogonal sequences.

5.1. Methodology and Formulation

In order to describe the properties of the downlink and the uplink, the channel coefficient is estimated. The channel coefficient is a quantitative representation of the transmitted signal changes that take place during the transmission. As RFID typically operates at low data rates [14], a narrow band channel is assumed that is completely described by a single complex coefficient that accounts for the signal change in magnitude and phase. The estimation is based on the comparison of the received signal $\mathbf{r} \in \mathbb{C}^N$ with a known transmit signal $\mathbf{s} \in \{-1, 1\}^N$. Note that N denotes the number of samples of the sequence, i.e., the sequences are typically oversampled.

When there is just one tag and therefore one channel, the WISP sends out a known sequence $\mathbf{s}_1 \in \{-1, 1\}^N$. Since the WISP reflects the reader signal, the channel coefficient $h \in \mathbb{C}$ is composed of a forward coefficient $h^{(f)}$(reader to tag) and a backward coefficient $h^{(b)}$ (tag to reader) such that $h = h^{(f)}h^{(b)}$. The received signal is composed of the carrier level c_1 of the reader and the transmitted signal $\mathbf{s}_1$ by tag taking into account the changes introduced by the channel h_1 (Equation 5.1). The channel estimation under perfect conditions is described in Equation 5.2. Note that a zero mean sequence is utilized, i.e., $\overline{\mathbf{s}_1} = 0$. Under realistic conditions, the estimation will be impaired by additive noise, and $\overline{\mathbf{s}_1}$ will be nonzero due to jitter. It should be noted that $< \mathbf{s}_1, \mathbf{s}_1 >= N$.

$$\mathbf{r}_1 = \mathbf{1}c_1 + \mathbf{s}_1 h_1 \tag{5.1}$$

$$\hat{h}_1 = \frac{1}{N} < \mathbf{s}_1, \mathbf{r}_1 >= \frac{1}{N}\left(\underbrace{\mathbf{s}_1^T\mathbf{1}}_{\overline{\mathbf{s}_1}} c_1 + \underbrace{\mathbf{s}_1^T\mathbf{s}_1}_{N} h_1\right) = \frac{1}{N}\overline{s_1}c_1 + h_1 = h_1 \tag{5.2}$$

In a multiple tag scenario there are as many channels as tags. In the case of two channels, orthogonal sequences $\mathbf{s}_1$ and $\mathbf{s}_2$ that satisfy $< \mathbf{s}_1, \mathbf{s}_2 >= 0$ are used. In this case the received signal comprises two contributions, one of each tag, as shown in Equation 5.3.

$$\mathbf{r} = \underbrace{\mathbf{s}_1 h_1 + \mathbf{1}c_1}_{\text{Tag 1}} + \underbrace{\mathbf{s}_2 h_2 + \mathbf{1}c_2}_{\text{Tag 2}} \tag{5.3}$$

The channel estimation for each channel, depicted in Equation 5.4 and Equation 5.5 for perfect conditions, is performed in the same way as in the one tag scenario.

№Sequence	Bit sequence	Miller-2 Encoding	Orthogonal Sequences
1	0 0 0 0	[1,-1, 1,-1,-1, 1,-1, 1, 1,-1, 1,-1,-1, 1,-1, 1]	6, 7, 11, 16
2	1 0 0 0	[1,-1,-1, 1,-1, 1,-1, 1, 1,-1, 1,-1,-1, 1,-1, 1]	5, 15
3	0 1 0 0	[1,-1, 1,-1, 1,-1,-1, 1,-1, 1,-1, 1, 1,-1, 1,-1]	9, 14
4	1 1 0 0	[1,-1,-1, 1,-1, 1, 1,-1, 1,-1, 1,-1,-1, 1,-1, 1]	6, 13
5	0 0 1 0	[1,-1, 1,-1,-1, 1,-1, 1,-1, 1, 1,-1, 1,-1, 1,-1]	2, 12
6	1 0 1 0	[1,-1,-1, 1,-1, 1,-1, 1,-1, 1, 1,-1, 1,-1, 1,-1]	1, 4, 11, 6
7	0 1 1 0	[1,-1, 1,-1, 1,-1,-1, 1,-1, 1, 1,-1, 1,-1, 1,-1]	1, 10
8	1 1 1 0	[1,-1,-1, 1,-1, 1, 1,-1, 1,-1,-1, 1,-1, 1,-1, 1]	9, 14
9	0 0 0 1	[1,-1, 1,-1,-1, 1,-1, 1, 1,-1, 1,-1, 1,-1,-1, 1]	3, 8
10	1 0 0 1	[1,-1,-1, 1,-1, 1,-1, 1, 1,-1, 1,-1, 1,-1,-1, 1]	7, 16
11	0 1 0 1	[1,-1, 1,-1, 1,-1,-1, 1,-1, 1,-1, 1,-1, 1, 1,-1]	1, 6, 13, 16
12	1 1 0 1	[1,-1,-1, 1,-1, 1, 1,-1, 1,-1, 1,-1, 1,-1,-1, 1]	5, 15
13	0 0 1 1	[1,-1, 1,-1,-1, 1,-1, 1,-1, 1, 1,-1, 1,-1,-1, 1]	4, 11
14	1 0 1 1	[1,-1,-1, 1,-1, 1,-1, 1,-1, 1, 1,-1, 1,-1,-1, 1]	3, 8
15	0 1 1 1	[1,-1, 1,-1, 1,-1,-1, 1,-1, 1, 1,-1, 1,-1,-1, 1]	2, 12
16	1 1 1 1	[1,-1,-1, 1,-1, 1, 1,-1, 1,-1,-1, 1,-1, 1, 1,-1]	1, 6, 10, 11

Table 5.1.: Milller-2 orthogonal sequences

$$\begin{aligned}\hat{h}_1 = \frac{1}{N} < \mathbf{s}_1, \mathbf{r}_1 > &= \frac{1}{N}\left(\underbrace{\mathbf{s}_1^T\mathbf{s}_1}_{N} h_1 + \underbrace{\mathbf{s}_1^T\mathbf{1}}_{\overline{\mathbf{s}_1}} c_1 + \underbrace{\mathbf{s}_1^T\mathbf{s}_2}_{0} h_2 + \underbrace{\mathbf{s}_1^T\mathbf{1}}_{\overline{\mathbf{s}_1}} c_2\right) \\ &= h_1 + \overline{\mathbf{s}_1}c_1 + \overline{\mathbf{s}_1}c_2 = h_1\end{aligned} \tag{5.4}$$

$$\begin{aligned}\hat{h}_2 = \frac{1}{N} < \mathbf{s}_2, \mathbf{r}_2 > &= \frac{1}{N}\left(\underbrace{\mathbf{s}_2^T\mathbf{s}_2}_{N} h_2 + \underbrace{\mathbf{s}_2^T\mathbf{1}}_{\overline{\mathbf{s}_2}} c_2 + \underbrace{\mathbf{s}_2^T\mathbf{s}_1}_{0} h_1 + \underbrace{\mathbf{s}_2^T\mathbf{1}}_{\overline{\mathbf{s}_2}} c_1\right) \\ &= h_2 + \overline{\mathbf{s}_2}c_2 + \overline{\mathbf{s}_2}c_1 = h_2\end{aligned} \tag{5.5}$$

5.2. Sequence Generation for Miller Encoding

As explained above, orthogonal sequences are necessary to do the channel estimation with CDMA. Since the WISP supports Miller encoding, in Table 5.1 are shown the orthogonal sequences of 4 bits related to Miller 2 encoding. Since Miller 2 encodes each bit with 4 symbols, each sequence is composed of 16 symbols.

As explained in the previous chapter, WISP 2 exhibits a significantly different clock frequency compared to WISP 1 and WISP 3. For this reason the WISP 2 is discarded for the channel estimation with orthogonal sequences. Therefore, just two orthogonal sequences will be necessary. The WISP 1 will reply with the sequence n$^{\underline{0}}$ 6 and the WISP 3 with the n$^{\underline{0}}$ 16, both mutually orthogonal.

5.3. Measurement Setup

For the channel estimation is used the Setup 2 explained in section 4.1. But this time, the WISP is attached to a moving support in order to do a position sweep. As shown in Figure 5.1, position 0 corresponds to the position where the tag is just in front of the reader.
When measurements with a single WISP are performed, it is placed vertically on the moving support (antenna aligned with the 0 position). In case of measurements with two WISPs, they are placed horizontally one above the other (center is aligned with the 0 position). For each position are measured 100 repetitions of the query.

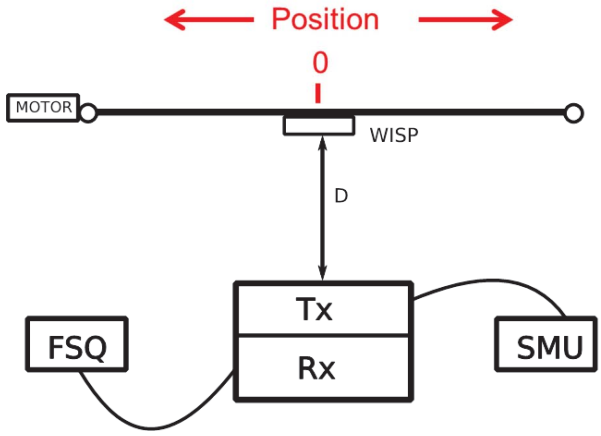

Figure 5.1.: Setup 2: Channel estimation

5.4. Firmware Changes

Definition of the commands

Instead of using the EPC commands, three kinds of query from the reader are defined:

- ***Query 1***: When it is sent, just WISP 1 replies.
- ***Query 3***: When it is sent, just WISP 3 replies.
- ***Query Both***: When it is sent, both WISPs reply.

Transmit code

In order to implement an orthogonal sequence response on the WISP, the transmit code (of the available firmware) is modified. This code is written in assembly. The first step is to delete the preamble and the end of signaling. Just one dummy bit is kept in order to detect the final bit of the response. The modified response is is shown in Figure 5.2. But as explained in Chapter 4, the DCOs of the WISPs do not have the same frequency, so the sequences will not be orthogonal. As found in Chapter 4, WISP 2 exhibits the slowest DCO frequency while WISP 3 features the fastest DCO frequency.

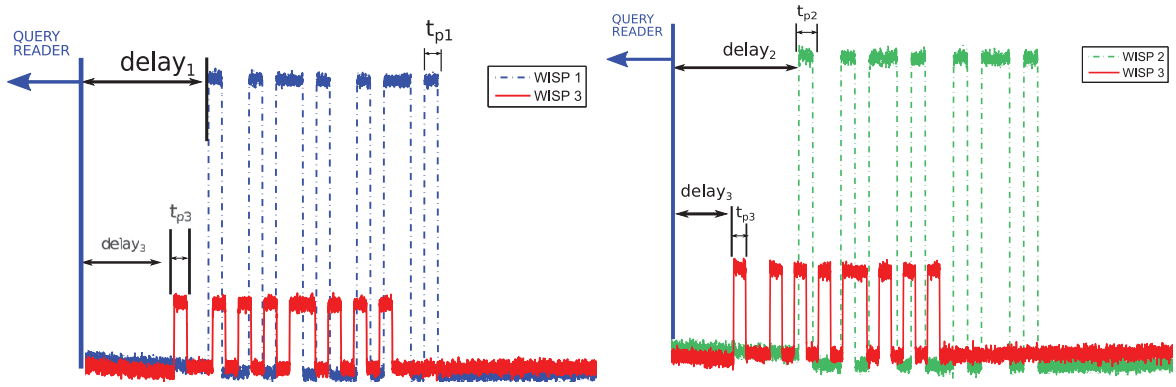

(a) Response WISPs 1 and 3

(b) Response WISPs 2 and 3

Figure 5.2.: Synchronization with the original firmware without preamble and end of signaling, and with a dummy data at the end

The initial delay is controlled with a timer. By changing the value of such timer the initial delay can be adjusted. The WISP 2 is discarded due to the large frequency deviation of its DCO. The response after adjusting the initial delay of WISP 1 and 3 is shown in Figure 5.3.

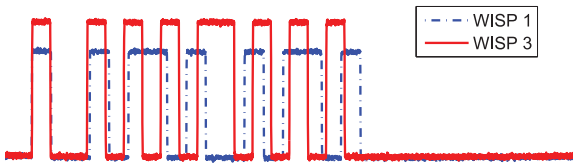

Figure 5.3.: Synchronization after adjusting the initial delay. Response WISPs 1 and 3

Now the pulse width must be adjusted. The operation of the transmit code is depicted in Figure 5.4. The timer counts up to the number stored in the register TACCR, and when it reaches that value the polarity of the transmit signal is flipped and the counter is reset. Since the WISP 3 has a faster DCO and therefore a shorter pulse width, the number in its TACCR register is increased. But, as the TACCR register value in the standard firmware is small, increasing by 1 the value of the register makes the pulse width 20% larger. Consequently, by increasing the register value in the WISP 3, the pulse width of the WISP 3 would be much bigger than that of WISP 1. In order to do a fine adjustment the threshold in both WISPs is doubled. It should be noted that empty cycles in assembly should be included. In this way, the pulses double their width and the backscatter link frequency is divided by two. This operation is depicted in Figure 5.4. The DCO is set to the range [0.54, 1.06] MHz. With this modification, the Backscatter Link Frequency (BLF) is 104.17 KHz, therefore the datarate is $\frac{104.17 \cdot 10^3}{4} = 26.0425\,\mathrm{kB/s}$. As every bit received or transmitted requires some computation, the clock rate is much higher than the bit rate. A finer adjustment and hence better synchronization would be possible if the TACCR register value is further increased. However, by keeping the DCO frequency constant, this results in a further reduction of the BLF and, consequently, the bit rate.

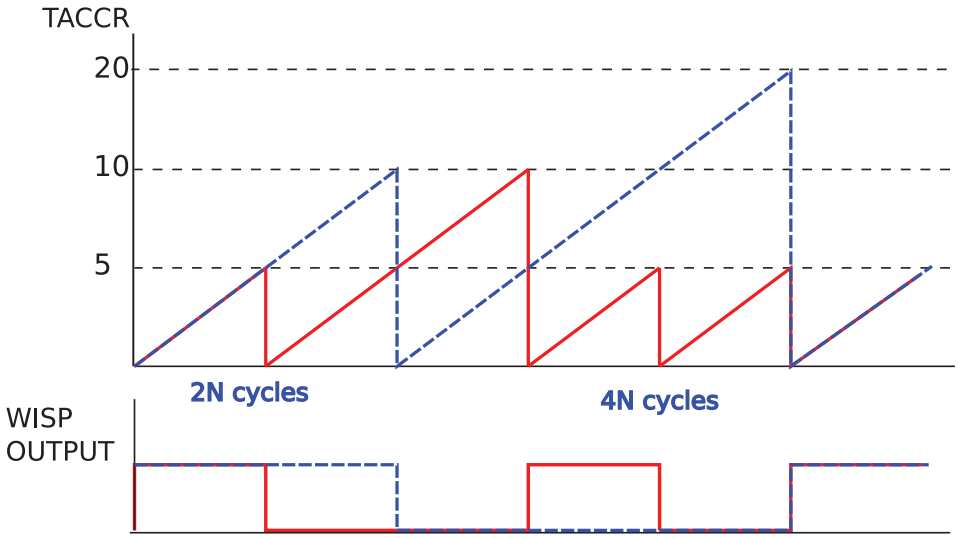

Figure 5.4.: Original and modified output

After adjusting the initial delay and the pulse width, the best synchronization achieved is shown in Figure 5.5.

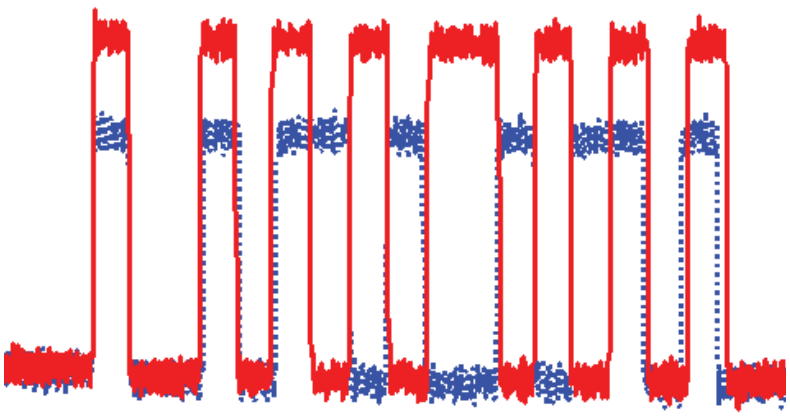

(a) Synchronization achieved (Query 1 (blue) and Query 3 (red))

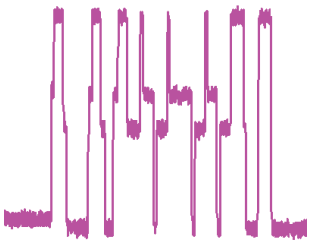

(b) Synchronization achieved (Query Both)

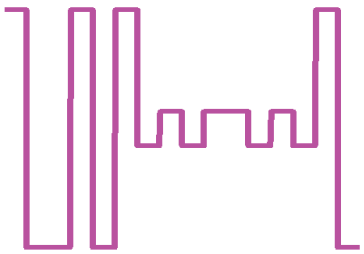

(c) Ideal synchronization

Figure 5.5.: Synchronization achieved after the software modifications

5.5. Single WISP

The setup for this measurement was explained above (see Figure 5.1), and the distance from the reader corresponding to position 0 is shown in Figure 5.6. For this measurements $P_{TX} = 25\,\text{dBm}$ and $f = 863\,\text{MHz}$.

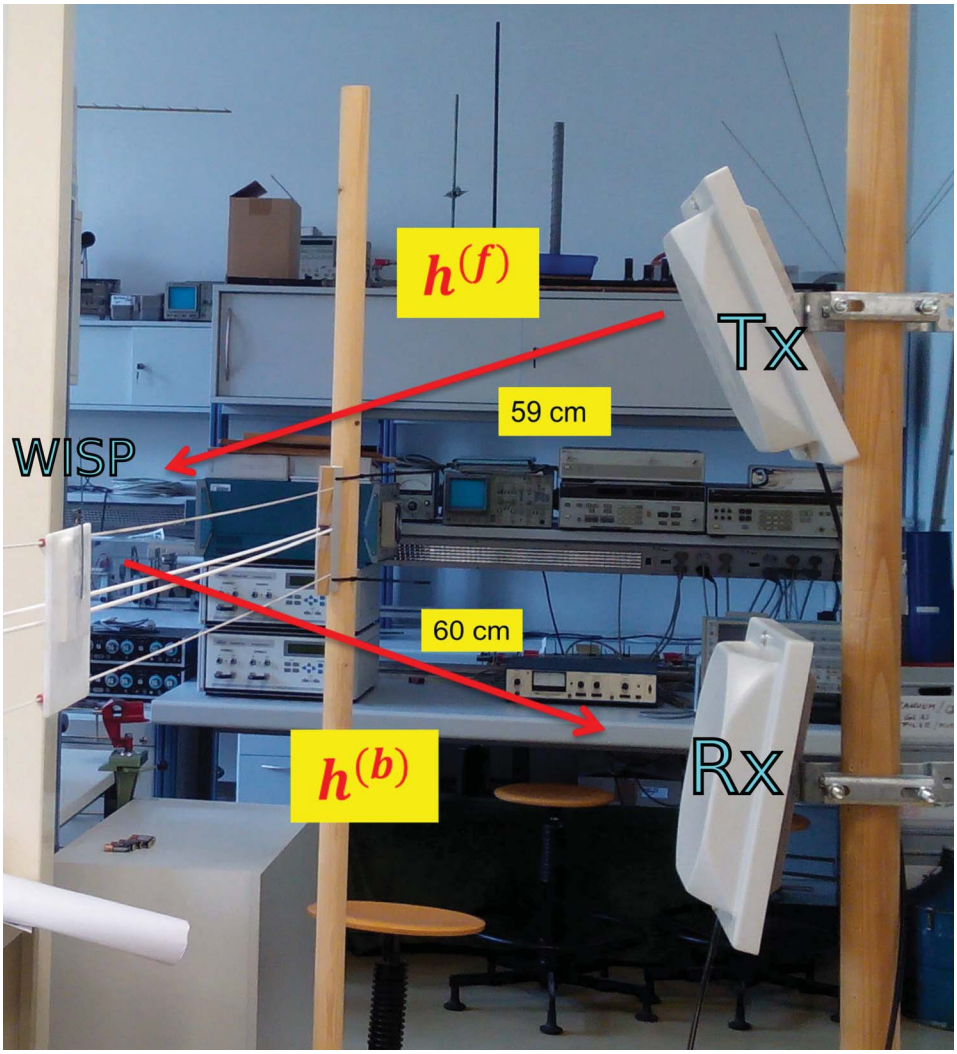

Figure 5.6.: Setup 2 for channel estimation with one WISP

In each position 100 repetitions are carried out, but the WISP does not respond always, so a probability of success can be defined as the number of times the WISP replies divided by the total number of querys sent by the reader. In this way, each position has a probability of success, plotted in Figure 5.7.

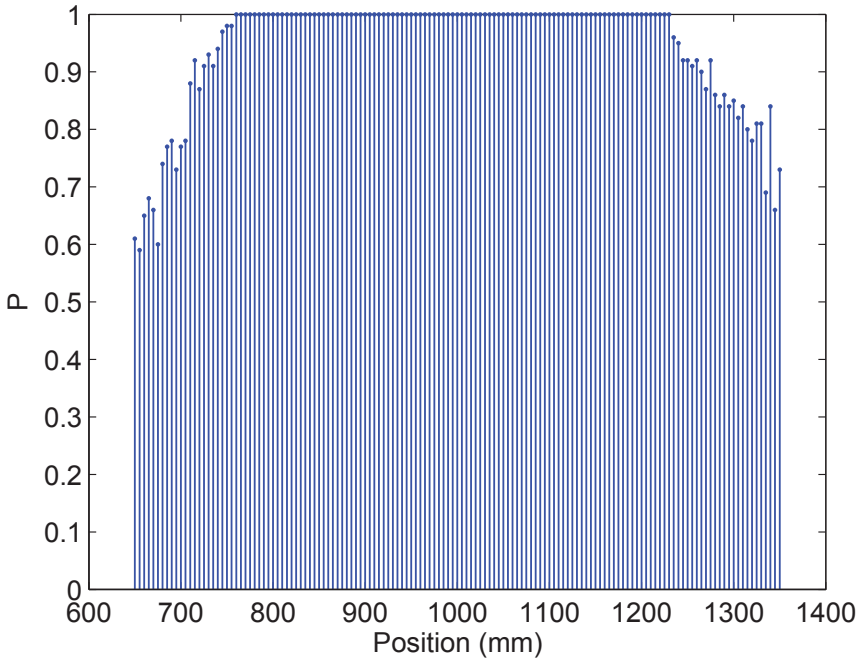

Figure 5.7.: Probability of success

The mean (over repetitions) of the magnitude and phase of the estimated channel coefficient in each position are plotted in Figure 5.8. Together with the magnitude, the standard deviation is plotted, but it is so small that it can be concluded that the channel coefficient is constant over the time for one fixed position. In Figure 5.8 is also depicted the channel coefficient in the complex plane. The darker points are related to the position closer to the left side (position= -350), and they become lighter when the WISP is moved to the right side (position= 350).

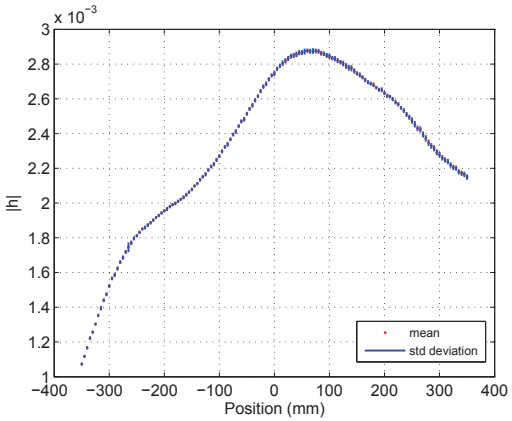

(a) Magnitude

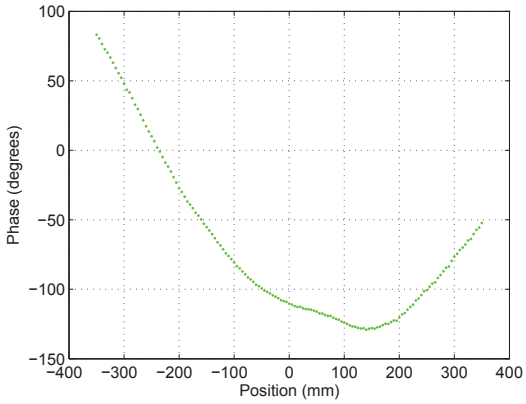

(b) Phase

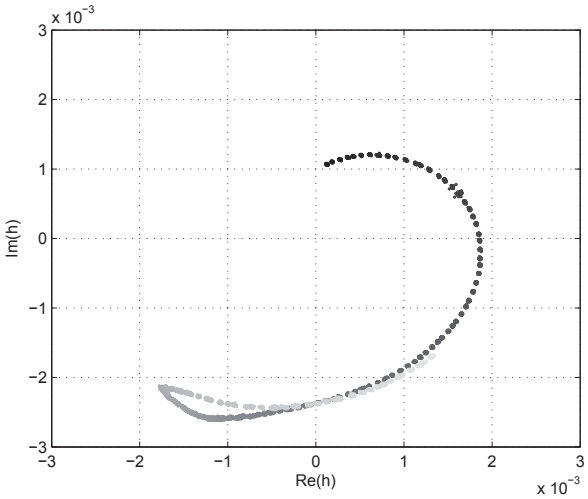

(c) IQ data

Figure 5.8.: Channel coefficient

On the other hand, as illustrated by Figure 5.9, after the query response the reader keeps on sending the carrier for a period of time defined by the signal generator. The mean of the carrier $\mathbf{c} \in \mathbb{R}^N$ in each position is estimated as

$$\hat{c} = \frac{1}{N} \sum_{i=1}^{N} c_i \tag{5.6}$$

and its variance is estimated as

$$\hat{\sigma}_n^2 = \frac{1}{N} \sum_{i=1}^{N} (c_i - \hat{c})^2. \tag{5.7}$$

The results are plotted in Figure 5.10.

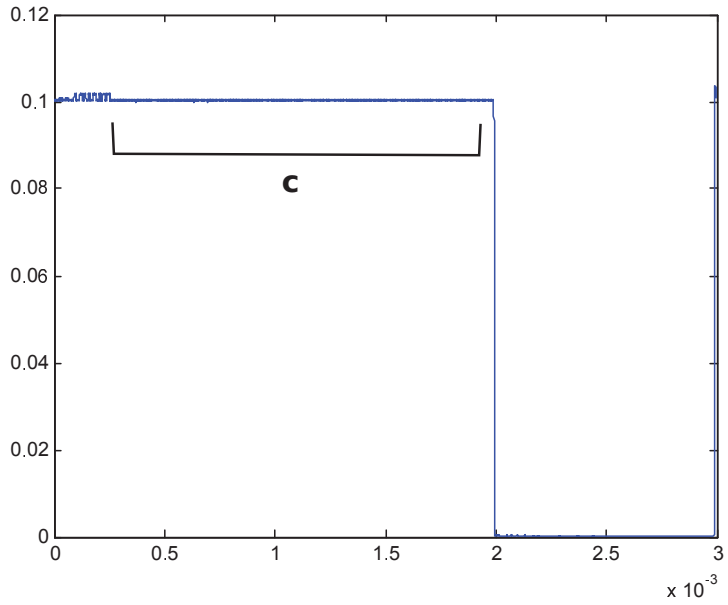

Figure 5.9.: Analysis of the carrier

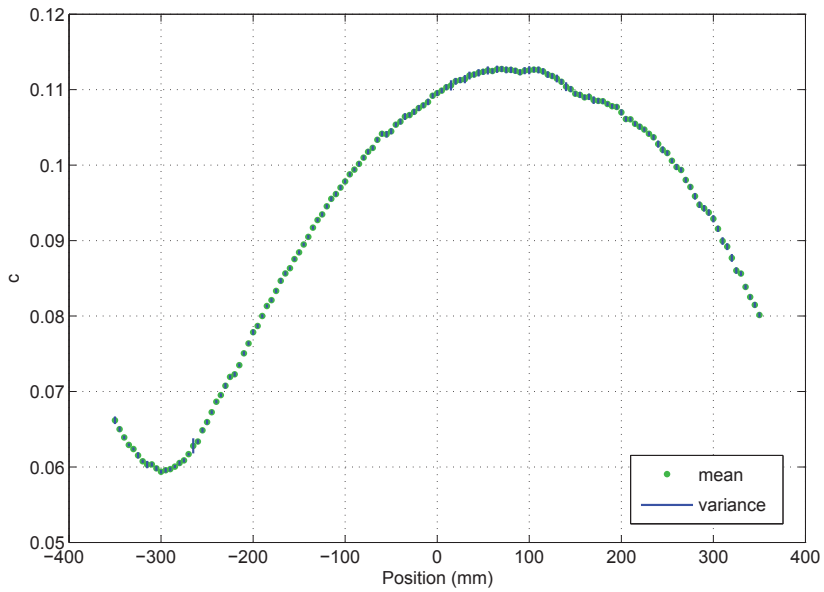

Figure 5.10.: Estimation of the mean and variance of the carrier

5.6. Multiple WISPs

Using setup 2, the distance from the reader corresponding to position 0 is shown in Figure 5.11.

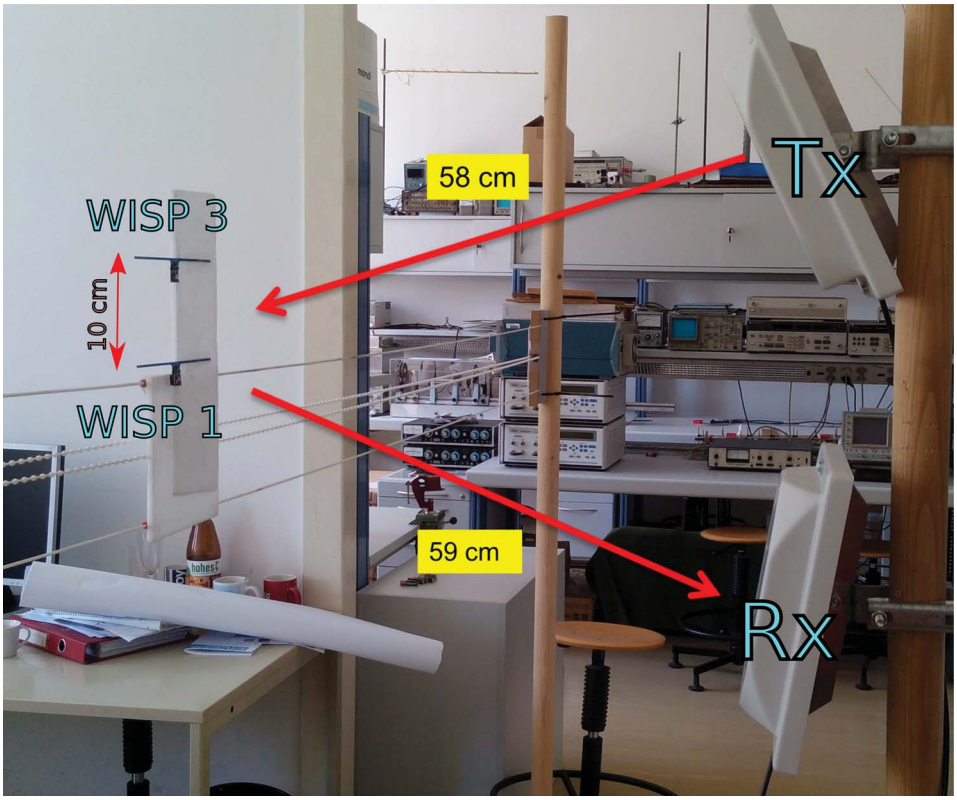

Figure 5.11.: Setup 2 for channel estimation with two WISPs

In this case, in each position the reader sends out the three kinds of query explained in section 5.4, each one 100 times. As in the previous case, the probability of success can be calculated but this time there will be a probability of success for each kind of query. The probability of success when the WISPs are responding separated (Query 1, 3) is plotted in Figure 5.12. Apart from not responding sometimes, the WISP can misunderstand the query from the reader and it might reply when the reader is not asking for its identification sequence. That might be because *Query 1* and *Query 3* just differ in one bit. On the other hand, the probability of success of WISP 3 is higher because it is closer to the transmit antenna and therefore it receives more power.

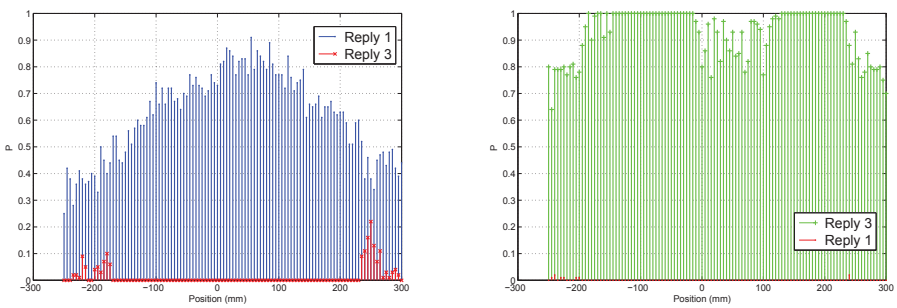

(a) Query 1

(b) Query 3

Figure 5.12.: Probability of success when the WISPs respond separately

When the reader sends a *Query Both*, WISP 1 and WISP 3 should reply, but as shown in Figure 5.13 sometimes just one single WISP replies.

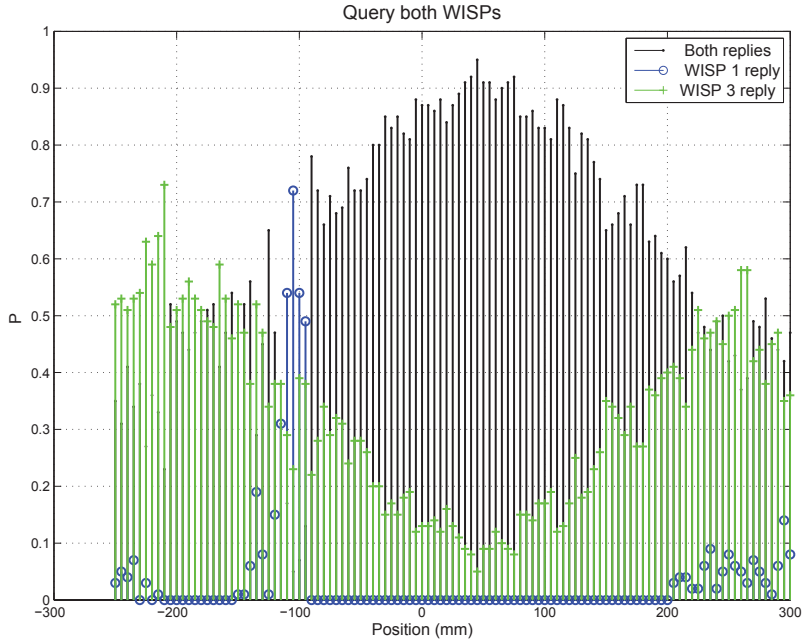

Figure 5.13.: Probability of success when the WISPs respond at the same time

The channel coefficients are shown in Figure 5.14. Though the WISP 3 receives more power, the backscattered signal of WISP 1 seems to be larger since it is closer to the receive antenna. Note that only the successful replies where considered in the channel estimation.

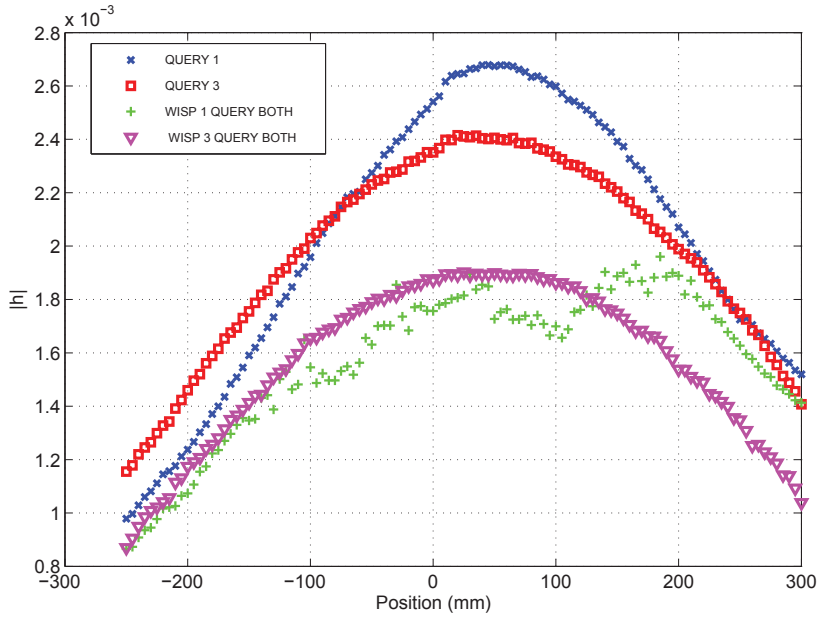

(a) Magnitude

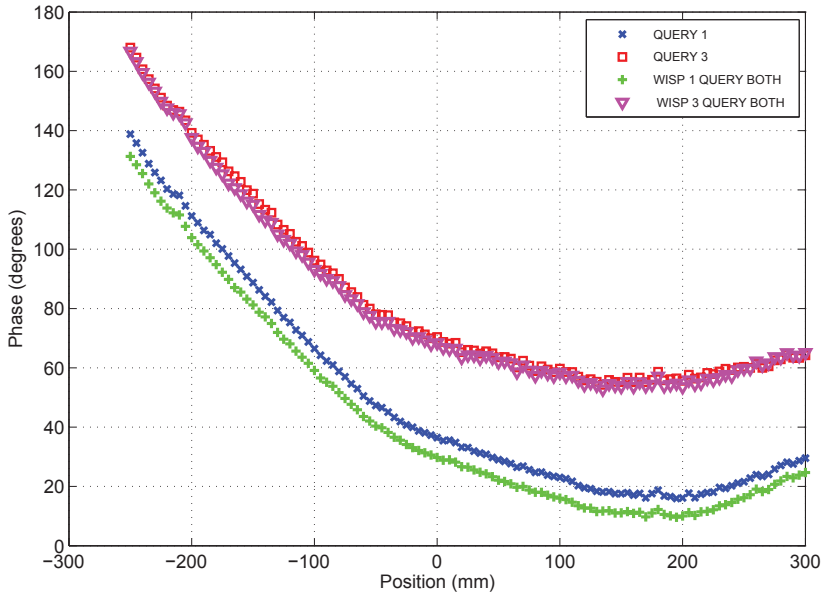

(b) Phase

Figure 5.14.: Channel coefficients

The mean of the carrier for each position is plotted in Figure 5.15. The mean in each position for the three kinds of query is practically the same.

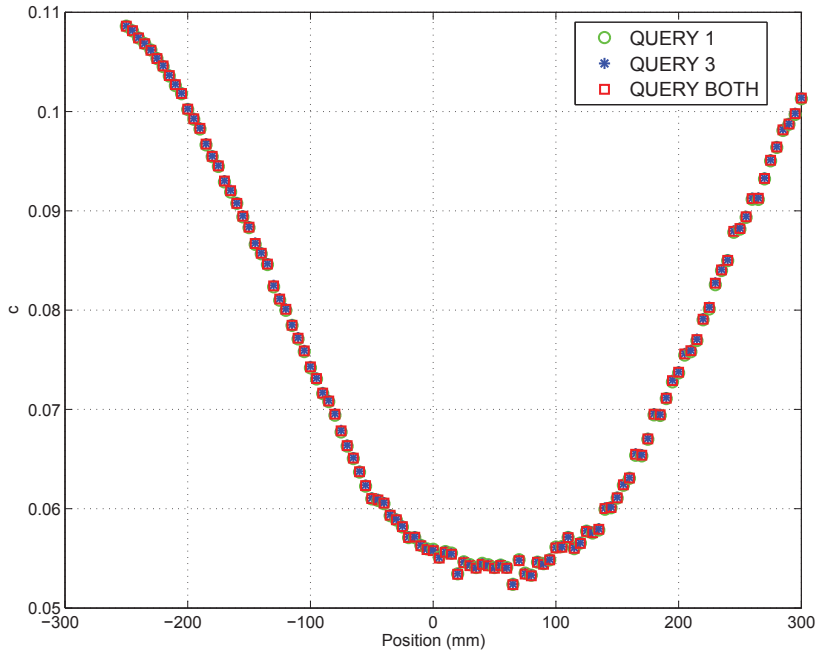

Figure 5.15.: Estimation of the carrier mean for several WISPs

The channel estimation of WISP 3 when both WISPs are responding is similar to the channel coefficient when just WISP 3 responds. But the channel estimation with WISP 1 is worse. To find out the reason, two consecutive positions with a big difference in the channel coefficient are selected. For example, the positions corresponding to -25 mm and -30 mm, as illustrated by Figure 5.16.

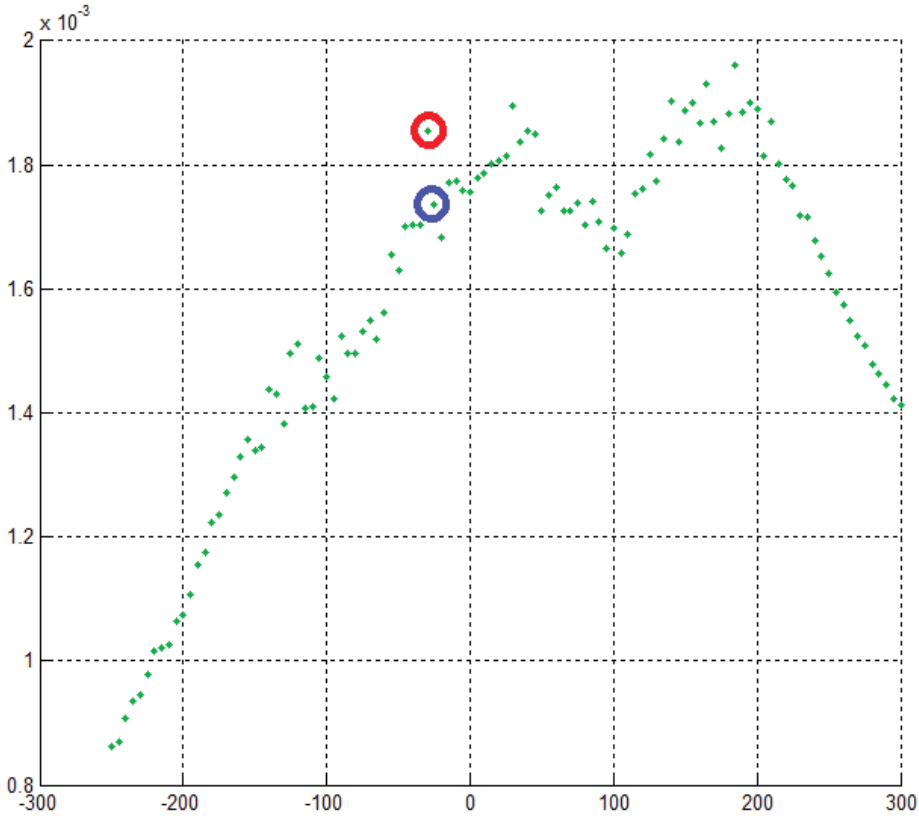

Figure 5.16.: Channel coefficient of WISP 1 when both platforms are responding at the same time. The positions corresponding to -25 mm and -30 mm are marked.

Now the value of the channel coefficient over the time of such positions is examined in Figure 5.17. Approximately, the channel coefficient can take three different values. The lower value is when the WISP 1 is not responding properly. In order to find out the differences between the remaining values, the complete WISP response for one particular repetition is examined. It should be noted that when the values of the channel coefficient are below 0.5×10^{-3}, it is because the WISP is not responding.

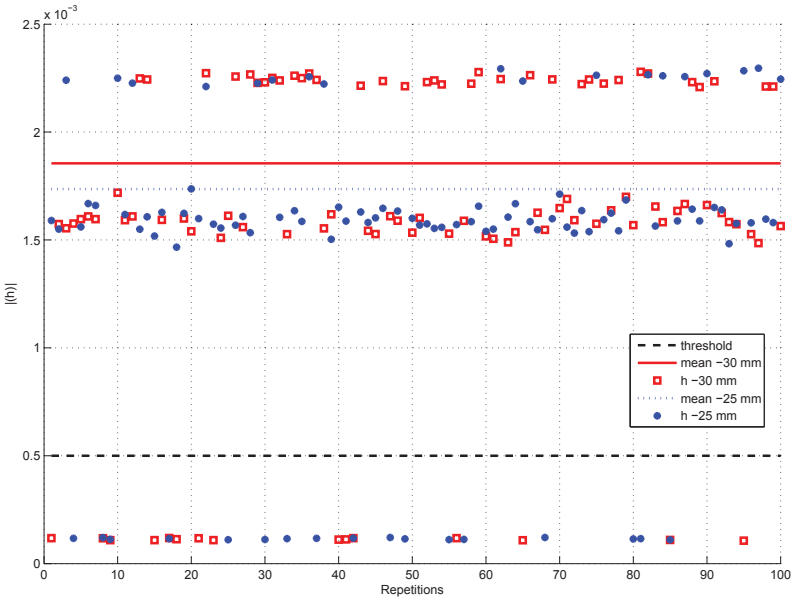

Figure 5.17.: Channel coefficient over the time for the position corresponding to -25 mm and -30 mm.

For the position −25 mm, repetitions 1 and 2 have a similar channel coefficient while the coefficient of repetitions 1 and 3 is quite different. The WISP reply (both WISPs reply simultaneously) related to the repetition 1 and 2 is plotted in Figure 5.18. These responses are almost identical. On the other hand, the WISP reply for repetition 1 and 3 is plotted in Figure 5.19. In this case the responses are not so similar. So it can be concluded that the channel estimation of the WISP 1 when both WISPs are responding is due to the imperfect synchronization.

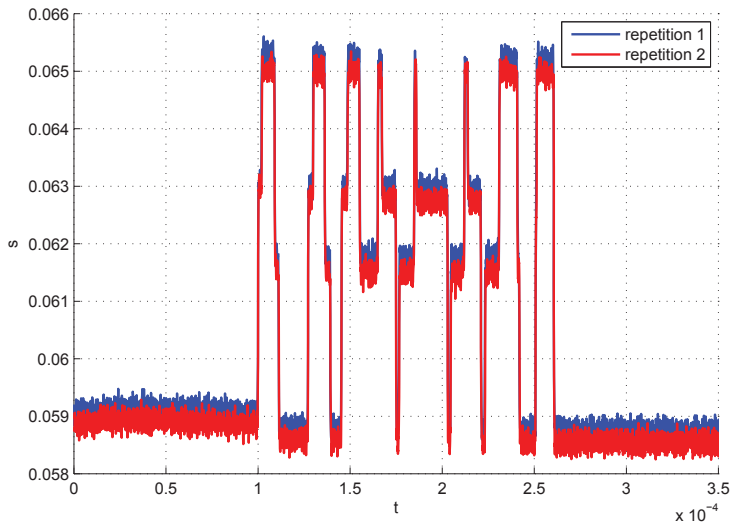

Figure 5.18.: WISP reply corresponding to position -25 mm (iterations 1 and 2)

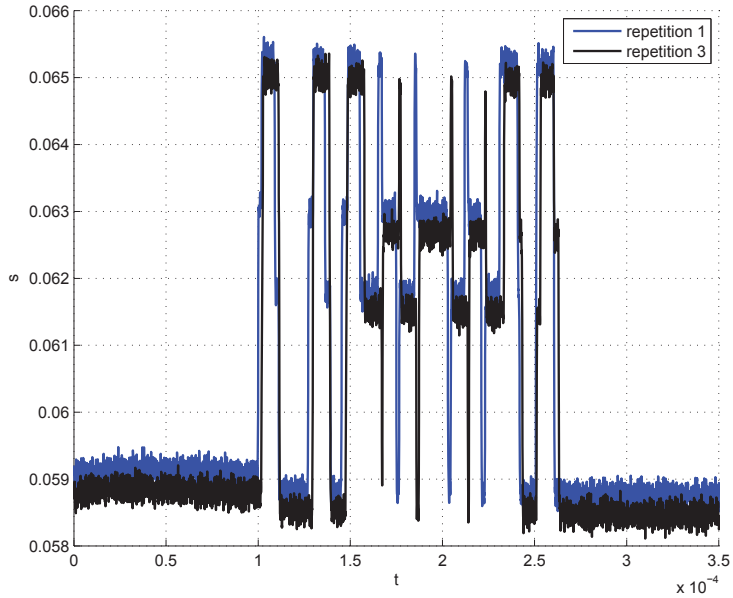

Figure 5.19.: WISP reply corresponding to position -25 mm (iterations 1 and 3)

Chapter 6.

Conclusion

In this thesis I investigated the Wireless Identification and Sensing Platform (WISP). Firstly, the antenna matching point in the UHF band, and the mutual influence of surrounding WISPs that may cause a mismatch in such point. Such influence is not very high, but the problem with multiple tag scenarios arises when the power up process is examined. The relation between the energy transmitted by the reader and the voltage the WISP received is strongly affected by others WISPs. The separation between two WISPs should be larger than 10 cm. It should be taken into consideration the distance from the reader to the WISPs, in order to achieve a read range in each WISP as similar as possible to the others WISPs.

The WISP internal clock has been investigated as well. Such clock is very imprecise and this leads to a link frequency deviation and, as a consequence, the WISP responses are not synchronized. As an advantage, the clock exhibits a insignificant jitter and its response does not change notably over the time. By software modification the synchronization between WISPs has been improved. Nonetheless, it is still far from an ideal synchronization and judging from the results, theoretical papers that are based on a perfect synchronization are far from being realizable. Some possible improvements are shown in Appendix A.

It also has been found that the WISP has a certain probability of success, i.e., it is not always responding. Also, the WISP response does not fade with the distance.

This thesis lays the foundation for developing new projects such as implementing custom identification protocols or developing sensing applications. It is also useful to get a feedback in order to build a customized tag, by getting rid of the WISP parts which are not necessary, depending on the application to build.

List of Figures

Bibliography

[1] D3.7 A Structured Collection on Information and Literature on Technological and Usability Aspects of Radio Frequency Identification (RFID), 2007. http://www.fidis.net/resources/fidis-deliverables/hightechid/int-d3700/doc/3/.

[2] K. Finkenzeller and D. Müller. *RFID Handbook: Fundamentals and Applications in Contactless Smart Cards, Radio Frequency Identification and Near-Field Communication*. Wiley, 2010.

[3] P.V. Nikitin and K.V.S. Rao. Antennas and Propagation in UHF RFID Systems. In *IEEE International Conference on RFID*, pages 277–288, April 2008.

[4] Syed A. Ahson and Mohammad Ilyas. *RFID handbook: applications, technology, security, and privacy*. CRC press, 2008.

[5] The different types of rfid systems. http://www.impinj.com//resources/about-rfid/the-different-types-of-rfid-systems.

[6] D.K. Klair, Kwan-Wu Chin, and R. Raad. A survey and tutorial of rfid anti-collision protocols. *Communications Surveys Tutorials, IEEE*, 12(3):400–421, Third 2010.

[7] Daeyoung Kim, M.A. Ingram, and Jr. Smith, W.W. Measurements of small-scale fading and path loss for long range RF tags. *IEEE Transactions on Antennas and Propagation*, 51(8):1740–1749, Aug 2003.

[8] *IAIK TU Graz*. https://www.iaik.tugraz.at/content/research/rfid/tag_emulators/.

[9] *18000-7 Active RFID Tags (IDENTEC SOLUTIONS)*. http://www.codesource.com/cat_name/active_rfid.aspx/.

[10] Tzu Hao Li, Alexey Borisenko, and Miodrag Bolic. Open platform semi-passive RFID tag. In *Ad-hoc, Mobile, and Wireless Networks*, pages 249–259. Springer, 2012.

[11] *WISP Wiki*. https://wisp.wikispaces.com.

[12] Daniel James Yeager. Development and Application of Wirelessly-Powered Sensor Nodes. Master's thesis, University of Washington, 2009.

[13] H. Zhang, J. J. Gummeson, B. A. Ransford, K. Fu. Moo: A Batteryless Computational RFID and Sensing Platform . Technical Report UM-CS-2011-0202, Computer Science, University of Massachusetts, June 2011.

[14] *EPCGlobal, EPC radio-frequency identity protocols class-1 generation-2 UHF RFID*. http://www.gs1.org/epcrfid/epc-rfid-uhf-air-interface-protocol/latest, May 2008.

[15] Jelena Kaitovic, Michal Šimko, Robert Langwieser, and Markus Rupp. Channel Estimation in Tag Collision Scenarios. In *IEEE International Conference on RFID*, pages 74–80. IEEE, 2012.

[16] Carlo Mutti and Christian Floerkemeier. CDMA-based RFID Systems in Dense Scenarios: Concepts and Challenges. In *RFID, 2008 IEEE International Conference on*, pages 215–222. IEEE, 2008.

[17] Joshua Y Maina, Marlin H Mickle, Michael R Lovell, and Laura A Schaefer. Application of CDMA for Anti-Collision and Increased Read Efficiency of Multiple RFID Tags. *Journal of Manufacturing Systems*, 26(1):37–43, 2007.

[18] Martin Mayer, Norbert Goertz, and Jelena Kaitovic. RFID Tag Acquisition via Compressed Sensing. In *RFID Technology and Applications Conference (RFID-TA), 2014 IEEE*, pages 26–31. IEEE, 2014.

[19] Jue Wang, Haitham Hassanieh, Dina Katabi, and Piotr Indyk. Efficient and reliable low-power backscatter networks. In *Proceedings of the ACM SIGCOMM conference on Applications, technologies, architectures, and protocols for computer communication*, pages 61–72. ACM, 2012.

[20] A.P. Sample, D.J. Yeager, P.S. Powledge, A.V. Mamishev, and J.R. Smith. Design of an RFID-Based Battery-Free Programmable Sensing Platform. *IEEE Transactions on Instrumentation and Measurement*, 57(11):2608–2615, Nov 2008.

[21] J.R. Smith. *Wirelessly Powered Sensor Networks and Computational RFID*. Springer New York, 2013.

[22] Alanson Sample, Daniel Yeager, Michael Buettner, Joshua Smith. *Development and Implementation of RFID Technology*. 2009.

[23] M. Philipose, J.R. Smith, B. Jiang, A. Mamishev, S. Roy, and K. Sundara-Rajan. Battery-free wireless identification and sensing. *Pervasive Computing, IEEE*, 4(1):37–45, Jan 2005.

[24] Texas Instruments. *MSP430x2xx Family User's Guide*. http://www.ti.com/lit/ug/slau144j/slau144j.pdf.

[25] Texas Instruments. *MSP430F2132 Data Sheet*. http://www.ti.com/lit/ds/symlink/msp430f2132.pdf.

[26] *WISP 5 Wiki*. https://wisp5.wikispaces.com/WISP+Home.

[27] Rohde & Schwarz GmbH & Co. KG. *R & S SMU200A Vector Signal Generator Operating Manual*. http://www.rohde-schwarz.com/en/product/smu200a-productstartpage_63493-7555.html, 2012.

[28] L.W. Mayer, M. Wrulich, and S. Caban. Measurements and Channel Modeling for Short Range Indoor UHF Applications. In *First European Conference on Antennas and Propagation (EuCAP)*, pages 1–5, Nov 2006.

[29] Agilent Technologies. *Agilent 34410A/11A 6 1/2 Digit Multimeter User's Guide*, 2012.

[30] Rohde & Schwarz GmbH & Co. KG. *R&S FSQ Signal Analyzer Operating Manual*. http://www.rohde-schwarz.com/en/product/fsq-productstartpage_63493-7994.html, 2014.

[31] *UBIK-808(ALN) UHF Inlay label*. http://www.rfidconnect.com/productdetails.aspx?id=5eca1858-fcb8-4bab-90d2-c1179b775447.

Appendix A.

Synchronization Improvements

Since the WISP DCOs are very imprecise, the synchronization to achieve orthogonal sequences is difficult to manage. Because of that, some possible improvements are proposed below.

Field-Programmable Gate Array (FPGA) as external clock

The microprocessor MSP430F2132 [25, 24] has the possibility to operate with an external signal clock. But on the WISP, such input for an external clock is not available since it is already used for an other purpose. In order to simulate an external clock signal, an FPGA is used. The setup is depicted in Figure A.1. In such setup, instead of transmitting the data stored on the WISP memory, the WISP transmits the data coming from the FPGA. This allows to convey very long responses, even if the WISP memory is not big enough to store the data. The clock signal coming from the FPGA is processed on the WISP as an interrupt. Each time that there is a rising edge, the WISP reads the data of the FPGA and sends out the same data (see Figure A.2). Note that the FPGA outputs the data with the falling edge, while the WISP loads the data with the next rising edge. This takes several clock cycles and since the internal WISP clocks are different the delay between the rising edge and the WISP output is different. But as explained in section 5.4, the initial delay is controlled with a timer and it is easy to modify.

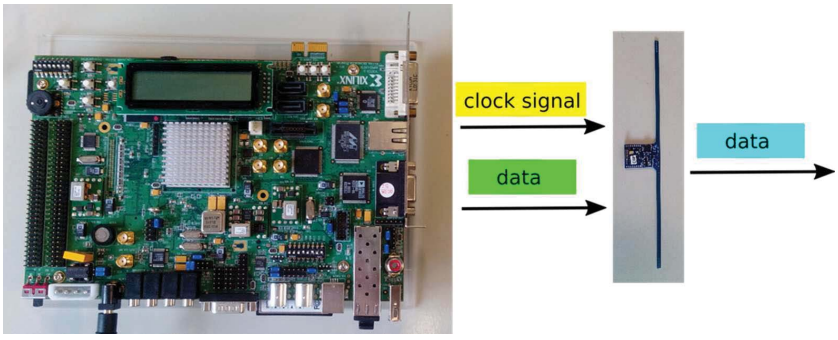

Figure A.1.: FPGA as an external clock setup

The pulse width problem is solved with this setup, but it has drawbacks: it is not wireless and the value of the timer to adjust the initial delay must be calculated individually for each WISP. Furthermore, a digital isolator has to be used between FPGA and WISP. This way, the WISP is decoupled from the FPGA board. Thus, it is still in passive operation and supplied by the reader.

Figure A.2.: Signals using an FPGA as an external clock: FPGA(yellow), FPGA data (green), WISP output (blue)

Hardware modifications

- **Use an external resistor for the Digitally Controlled Oscillator (DCO)**: the microcontroller MSP430F2132 provides the option to source the DCO current through an external resistor. This allows to tune the DCO frequency by changing the resistor value. Therefore, by susing accurate resistor values on all WISPs, the synchronization would improve. But this approach requires hardware modification.

- **Use an external crystal**: the WISP has already a crystal as one of the clock sources that can be selected (see section 2.2), but it has a very low frequency. As the data rate is much lower than the clock rate, the BLF using such crystal would be very low. A new crystal could be used as an external clock (HF clock) in order to achieve a more accurate frequency. But this option requires a new WISP design.